CORA Cork Open Research Archive
Cartlann Taighde Oscailte Chorcaí

Title	Spectral stability of solutions to Whitham-type equations with a nonlocal kernel
Authors	McCormack, Kathleen Tamarisk
Publication date	2024
Original Citation	McCormack, K. T. 2024. Spectral stability of solutions to Whitham-type equations with a nonlocal kernel. MSc Thesis, University College Cork.
Type of publication	Masters thesis (Research)
Rights	© 2024, Kathleen Tamarisk McCormack. - https://creativecommons.org/licenses/by/4.0/
Download date	2026-11-02 23:09:01
Item downloaded from	https://hdl.handle.net/10468/17498



UCC
University College Cork, Ireland
Coláiste na hOllscoile Corcaigh



ucc

Coláiste na hOllscoile Corcaigh, Éire
University College Cork, Ireland

Spectral stability of solutions to Whitham-type equations with a nonlocal kernel

Kathleen Tamarisk McCormack

117460154

UNIVERSITY COLLEGE CORK

SCHOOL OF MATHEMATICAL SCIENCES

Supervisor:

Dr Kieran Mulchrone

Head of School:

Dr Kevin Hayes

Master of Science - 2024

Abstract

This thesis aims to provide a clear and reproducible outline of finding travelling wave solutions to certain nonlinear partial differential equations. This is done using a spectral cosine collocation method, and the stability of the travelling wave solutions found is then assessed using the Fourier-Floquet-Hill method. This is first done on a number of examples. Next, a variation of the Whitham equation which uses a nonlocal kernel with a parameter ν, that determines the strength of the dispersion, was solved and its stability spectra analyzed. This model is expected to have both stable continuous solutions and unstable breaking solutions, depending on the parameter ν.

The solution method worked well across all examples and replicated prior results. It was less effective for the cases of the nonlocal modified dispersion model where breaking solutions would occur. This is due to a limitation in the assumptions of the Fourier method. The stability analysis aligned with previous findings for the cubic vortical Whitham equation and showed that the solutions that were found for the nonlocal modified dispersion model were stable. Further research is needed to assess the stability of the breaking solutions, which this solution method did not capture.

Acknowledgements

I would like to extend my thanks to my supervisor Kieran Mulchrone for all the support and guidance over the years. I would also like to thank Mick Mortell for his invaluable insight at the outset of this project.

Declaration of Independence

This is to certify that the work I am submitting is my own and has not been submitted for another degree, either at University College Cork or elsewhere. All external references and sources are clearly acknowledged and identified within the contents. I have read and understood the regulations of University College Cork concerning plagiarism and intellectual property.



Kathleen Tamarisk McCormack
16/09/2024

Table of Contents

List of Figures **5**

1 Introduction **7**

2 Finding solutions - spectral methods **12**

2.1 Background to spectral methods 12

2.2 Derivation of discrete cosine transform and its inverse 13

2.3 Discrete cosine transform in MATLAB 17

2.4 Differentiation matrices 18

2.5 Newton's method 20

2.6 Applications 21

2.6.1 Korteweg-deVries and Burgers equation 21

2.6.2 Whitham-Burgers equation 26

2.6.3 Whitham equation 31

2.6.4 Cubic-Vortical Whitham equation 34

2.7 Alternative Fourier solution method 36

3 Spectral stability of solutions - Fourier-Floquet-Hill method **40**

3.1 Fourier-Floquet-Hill method 40

3.2 Cubic-Vortical Whitham equation 42

4 CV-Whitham equation computational results **50**

5 Modified Dispersion Whitham equation **55**

5.1 Derivation 55

5.2 Comparison between linear phase speed of kernels 58

5.3 Solution results 60

5.4 Spectral stability results 63

6 Discussion and Conclusion **66**

6.1 Discussion 66

6.2 Conclusion 70

7 Appendices **75**

7.1 Mathematica code to solve the CV-Whitham equation and determine the stability of those solutions 75

7.2 Details on integration 80

List of Figures

1 Solution to the Burgers equation with wave speed $c = 2$. 24

2 Solutions to the KdV equation with wave speed $c = 1.5$ with differing initial guesses applied. 25

3 Solutions to the KdV-B equation with wave speed $c = 2$, and initial guess $\phi = 1 - \tanh(3(x - \frac{\pi}{2}))$. 26

4 Solutions to the Whitham-B and KdV-B equations with $c = 1.2$ and $\epsilon = 0.05$. 31

5 Solutions to the Whitham equation for varying values of c and continually updating initial guesses. 33

6 Solutions to the CV-Whitham equation with $L = 2\pi$, $\Omega = 0$, and various values of wave speed c. The calculated wave height of the solution is also given. 50

7 Plot of wave speed c versus wave height H for solutions of the CV-Whitham equation with $L = 2\pi$ and $\Omega = 0$. 51

8 Stability spectra for some solutions of the CV-Whitham equation with $L = 2\pi$ and $\Omega = 0$, where it is not enforced that the mean is zero, with their respective wave speeds c and wave heights h given. 52

9 Wave speed c versus the maximum real eigenvalue of the stability spectra, for solutions to the CV-Whitham equation with $L = 2\pi$ and $\Omega = 0$. 54

10 Plot of the linear phase speed $\tilde{c}$ against the wave number k for the Whitham, KdV, and MD-Whitham models, the latter done for values of $\nu = 2\pi, \pi, \frac{\pi}{2}, \frac{\pi}{4}, \frac{\pi}{8}$. 59

11 Solutions to the Whitham equation with a nonlocal kernel for $\nu = 2\pi$ 61

12 Solutions to the Whitham equation with a nonlocal kernel for $\nu = \frac{3\pi}{2}$ 62

13 Solutions to the Whitham equation with a nonlocal kernel for $\nu = \pi$. 62

14 Stability spectra of the representative solution to the MD-Whitham term for $\nu = 2\pi$ and $c = 1.2$. 65

15 Solution to the Heat equation progressing over time, found in the method described by Kutz and Brunton [5]. 67

16 Solution to the Burgers equation progressing over time, found in the method described by Brunton and Kutz [5]. 68

17 Solutions to the MD-Whitham equation for $\nu = \frac{\pi}{16}$ progressing over time, found in the method described by Brunton and Kutz [5] 69

1 Introduction

The primary aims of this thesis are to firstly give a lucid outline of how to compute solutions to Korteweg-deVries (KdV) type partial differential equations, using a spectral cosine collocation method, and secondly to determine the stability of these solutions, using the Fourier-Floquet-Hill method.

The following KdV-type wave equations are considered in this thesis, where η represents surface displacement, x represents space, and t represents time:

- the non-dimensional *KdV equation*: $\eta_t + \eta_x + \eta\eta_x + \frac{1}{6}\eta_{xxx} = 0$,
- the *Burgers equation*: $\eta_t + \eta\eta_x = \epsilon\eta_{xx}$, where ϵ is a small positive parameter that varies the strength of the dispersive term,
- the *KdV-B equation*, which combines the KdV and Burgers equations: $\eta_t + \eta_x + \eta\eta_x + \frac{1}{6}\eta_{xxx} = \epsilon\eta_{xx}$,
- the non-dimensional *Whitham equation*: $\eta_t + \eta\eta_x + K * \eta_x = 0$ where K is defined by the Fourier multiplier $\hat{K}(k) = \sqrt{\frac{\tanh(k)}{k}}$,
- the *Whitham-B* equation, which combines the Whitham and Burgers equations: $\eta_t + \eta\eta_x + K * \eta_x = \eta_{xx}$, where again $\hat{K}(k) = \sqrt{\frac{\tanh(k)}{k}}$,
- the *cubic vortical Whitham* or *CV Whitham* equation: $\eta_t + \mathcal{K} * \eta_x + \alpha\eta\eta_x + \beta\eta^2\eta_x = 0$ where $\hat{\mathcal{K}}(k) = -\frac{\Omega\tanh(k)}{2k} + \sqrt{\frac{\tanh(k)}{k} + \frac{\Omega^2\tanh^2(k)}{4k^2}}$, $\alpha = \frac{\Omega^2+3}{\sqrt{\Omega^2+4}}$, and $\beta = -\frac{6+\Omega^2}{2(4+\Omega^2)^{\frac{3}{2}}}$, and
- a *modified dispersion Whitham* equation or *MD-Whitham* equation: $\eta_t + \frac{3}{2}\eta\eta_x + K_\nu * \eta_x = 0$ where K_ν is defined by the Fourier multiplier $\hat{K}_\nu(k) = -k^2 e^{-\frac{k^2}{4\nu^4}}$.

The Korteweg-deVries (KdV) equation was first introduced in 1877 by Joseph Boussinesq [2][9], and rediscovered over a century later by the equation's namesakes Diederik Korteweg and Gustav deVries [9][20]. The KdV equation is known for

the fact that it has a soliton solution, which is made possible by the effects of its nonlinear and dispersive terms balancing each other out. Substituting a travelling wave ansatz into the KdV equation yields an ordinary differential equation with two solutions, the first a solitary wave (the soliton solution), and the second a cnoidal wave, so named because it is written in the form of the Jacobi elliptic function cn [26]. The soliton was first noted in 1834 by Scottish engineer John Scott Russell [27] who observed a barge, pulled by horses in the Union Canal near Edinburgh, come to a halt. He beheld that the wave at the bow of the boat continued to move forward, without loss of speed or change of shape, famously chasing it for several miles on horseback. He first called this "singular and beautiful phenomenon" a Wave of Translation. It was in 1965 that Zabusky and Krustal [32] coined the term "soliton" to describe this, and it is the KdV equation's soliton solutions that make it the subject of much fascination.

While the KdV is a good model for the long wave/shallow water case [6][28], its domain of validity is limited, thus requiring further variations of the model. One such variation is the Korteweg-deVries-Burgers (KdV-B) equation, named after the Burgers term from which it borrows a second derivative diffusive term [1]. This was originally put forward by Whitham (Ch.13.15, [31]) with the intent that the added dissipation would yield solutions featuring undular bores. It was proven that it did so by Bona and Schonbek [1], and these solutions were found numerically by Nevland [26] *inter alia*.

Whitham (Ch.13.14, [31]) proposed replacing the third derivative dispersion term of the KdV equation with a Fourier multiplier, referred to as a kernel. This equation is now known as the Whitham equation. While it has no known nontrivial solutions, it has been the subject of much research. Moldabayev et al. [24] formally derived the Whitham equation from the Hamiltonian theory of surface water waves, and compared the Whitham equation with the KdV and two other equations to determine which served best as a model for free surface dynamics. They found the Whitham model performed as well as or better than the other models investigated.

Ehrnström and Kalisch [11] proved the existence of non-trivial, small-amplitude, travelling wave solutions to the Whitham equation, and found approximate numerical solutions. Hur and Johnson [16] proved that periodic travelling wave solutions of the Whitham equation are spectrally unstable with respect to long-wavelength perturbations if the wavenumber exceeds a critical value, and are spectrally stable otherwise. This result was demonstrated by the numerical work of Sanford et al. [28], who state that all large-amplitude solutions are unstable, while small-amplitude solutions with sufficiently large wavelengths are stable. They concur with Hur and Johnson that periodic travelling wave solutions of the Whitham equation exhibit modulational instability when the wavelength is too small, the cut-off value for which is $kh_0 = 1.145$, where $k = \frac{2\pi}{L}$ is the wavenumber and h_0 is the mean undisturbed fluid depth.

Nevland [26] proposed that, if the Whitham equation is a better version of the KdV equation (in that it is also applicable to short wavelengths) and the KdV-B equation allows undular bore solutions, perhaps a Whitham-Burgers equation would be an improvement on the KdV-B equation. He specified that by "improvement" he means that it models more closely the presumed undular bore solutions of the Navier-Stokes equations. While the Navier-Stokes equations are dissipative models, i.e. they model energy loss, and this is required to yield undular bore solutions, they are too difficult to solve numerically to be a useful model. He found numerically, that the Whitham-B equation gives similar results as the KdV-B equation, but with stronger dispersion evident, which is consistent with the additional dispersion term that was included.

The cubic vortical Whitham (CV-Whitham) equation has been proposed as a generalisation of the vor-Whitham equation by Kharif et al. [19] and Kharif and Abid [18]. The vor-Whitham equation is not the focus here, but models two-dimensional nonlinear gravity waves travelling in shallow water on a vertically sheared current of constant vorticity [18]. The solutions and stability of the CV-Whitham equation are studied by Carter et al., who found that all moderate and large amplitude solutions

are found to be unstable, regardless of wavelength [6].

Hur [15] proved wave breaking for the Whitham equation, provided the initial data is sufficiently negative, and this result was generalised by Hur and Tao [17] to permit the Whitham equation bidirectional propagation. That which has here been referred to as the Modified Dispersion Whitham (or MD-Whitham) equation, was suggested by Mortell and Mulchrone [25], as a model that describes both breaking and continuous solutions. It replaces the kernel term proposed by Whitham by another, which includes a scaleable parameter ν, varying which, determines whether the solutions are continuous.

This thesis replicates the work of Nevland [26] in solving the KdV, Burgers, KdV-B, and Whitham-B equations, the work of Sanford et al. [28] in solving the Whitham equation, and the work of Carter et al. [6] in solving the CV-Whitham equation, using the cosine collocation method. This method is then used to solve the MD-Whitham equation proposed by Mortell and Mulcrone [25]. The stability of the solutions to the CV-Whitham equation (as done by Carter et al. [6]) and the MD-Whitham equation is then studied using the Fourier-Floquet-Hill method.

The remainder of this thesis is outlined as follows:

Chapter 2 details the solution method, giving the benefits of spectral methods, and deriving the spectral method used here. This includes the derivation of the discrete cosine transform and its inverse, as well as differentiation matrices. The history, benefits, and shortcomings of the equations listed above are stated and they are solved using the cosine collocation method. An alternative but equivalent solution method in terms of Fourier series is also discussed and this is implemented for the MD-Whitham equation.

Chapter 3 examines spectral stability analysis in detail, providing the history and outline of the Fourier-Floquet-Hill method. As an example, this method is then worked through explicitly for the case of the cubic vortical Whitham equation

[6], including details of how it can be applied similarly to the traditional Whitham equation. Computational considerations are also discussed.

Chapter 4 presents solutions of the cubic vortical Whitham equation computed here and compares them to published results. The spectral stability is computed for these solutions and they are found to consistent be with those from other studies.

Chapter 5 introduces the MD-Whitham equation, a variation on the Whitham equation that yields both continuous and breaking solutions [25]. This behaviour is facilitated by the introduction of a nonlocal kernel with a tuneable parameter (ν), the value of which controls the relative strength of the nonlinear and dispersive elements of the equation. The spectral cosine collocation method is used to find solutions, and the Fourier-Floquet-Hill method is used to determine their stability. The expectation is that continuous solutions will be stable, and breaking solutions unstable.

2 Finding solutions - spectral methods

2.1 Background to spectral methods

Popular ways of numerically solving partial differential equations (PDEs) include finite difference methods, finite element methods, and spectral methods. Spectral methods write the solution to a PDE as the sum of a number of basis functions and then choose the coefficients that solve the PDE best. Spectral collocation methods, which are also known as pseudospectral methods, are a subset of spectral methods based on using a high-order interpolating polynomial at the collocation points across the entire domain. In this way, they resemble finite difference methods, which also use collocation points. However, compared to finite difference methods, spectral methods achieve better accuracy over fewer points [8]. Spectral methods and finite element methods differ in that spectral methods use basis functions with support over the entire domain, whereas finite element methods use basis functions with local support [30].

A Fourier pseudospectral method may be used to solve many PDEs with periodic boundary conditions. For this, the PDE is transformed into Fourier space where it's derivative is easier to calculate, causing it to become a system of ODEs; this is then solved in the Fourier domain and the solution transformed back to the spatial domain. In some cases however, for example, where a nonlinear term is present, it is necessary to transform the system of ODEs back into the spatial domain to be solved. This is less computationally efficient but not egregiously so, and it is sometimes unavoidable. This Fourier pseudospectral is given some consideration in Section 6.1.

A related method of solving PDEs is a spectral cosine collocation method, which is in essence, a restriction of the Fourier collocation method to even functions. It relies on a cosine transform to provide differentiation matrices which are used in

place of differentiating in Fourier space. The next section provides details of the derivation of the discrete cosine transform.

2.2 Derivation of discrete cosine transform and its inverse

This derivation of the discrete cosine transform follows closely that of Nevland [26]. Consider a 2π-periodic function u that is integrable on $x \in [0, 2\pi]$. Its Fourier series expansion is given by

$$u(x) = \sum_{k=-\infty}^{\infty} \hat{u}_k(t) e^{ikx},$$

where $\hat{u}_k$ are the Fourier coefficients, defined as

$$\hat{u}_k(t) = \frac{1}{2\pi} \int_0^{2\pi} u(x,t) e^{-ikx} dx. \tag{1}$$

If the additional assumption is made that the function is even about π, then only a series of cosines remains. This can be seen by writing the series expansion in terms of sines and cosines, rather than e, and then noting that the Fourier coefficients of the sine terms will be zero (see Lemma 2.2 in Folland [12]). The function will now also be referred to as ϕ to keep the even function distinct from u, which was not necessarily even. Thus we have

$$\phi(x) = \sum_{k=0}^{\infty} a_k \cos(kx), \tag{2}$$

where the cosine coefficients a_k are related to the Fourier coefficients $\hat{\phi}_k$ in Eq. (1) by $a_0 = \hat{u}_0$ and $a_k = \hat{u}_k + \hat{u}_{-k}$.

Enforcing (2), the cosine series expansion of ϕ, at a number of collocation points provides our approximation for ϕ. Naturally, this cannot be done for an infinite number of points, so in practice, a truncation of Eq. (2) is applied. The collocation

points x_j used are defined as

$$x_j = \frac{(2j-1)\,\pi}{2N}, j = 1, ..., 2N+1. \tag{3}$$

Therefore the Fourier coefficients are given, similar to Eq. (1), as

$$\begin{aligned} \hat{\phi}_k(t) &= \frac{1}{2\pi} \int_{\frac{\pi}{2N}}^{2\pi+\frac{\pi}{2N}} \phi(x,t) e^{-ikx} dx \\ &= \frac{1}{2\pi} \int_{0}^{2\pi} \phi(x,t) e^{-ikx} dx \end{aligned} \tag{4}$$

Note that the limits of the integral used are $[0, 2\pi]$, despite the fact that the collocation points range from $\frac{(2(1)-1)\pi}{2N} = \frac{\pi}{2N}$ to $\frac{(2(2N+1)-1)\pi}{2N} = 2\pi + \frac{\pi}{2N}$. However, using the limits $[0, 2\pi]$ is equivalent to using the limits $\left[\frac{\pi}{2N}, 2\pi + \frac{\pi}{2N}\right]$, due to the following result:

Lemma 2.1 [12] If F is periodic with period P, then $\int_a^{a+P} F(x)dx$ is independent of a.

Proof: See Folland (pg. 21, Lemma 2.1) [12].

To define the transform involved, an approximation of the coefficients is required and is found by approximating the integral in (1) by the trapezoidal rule. The trapezoidal rule states

$$\int_a^b f(x)dx \approx \frac{\Delta x}{2} \left(f(x_0) + 2f(x_1) + 2f(x_2) + ... + 2f(x_{N-1}) + f(x_N) \right).$$

Applying this to the integral in Eq. (4) yields that

$$\begin{aligned}\int_0^{2\pi} \phi(x,t)e^{-ikx}dx &\approx \frac{\Delta x}{2}\left(\phi(x_1)e^{-ikx_1} + 2\phi(x_2)e^{-ikx_2}\right.\\ &\qquad \left. +\ldots + 2\phi(x_{2N})e^{-ikx_{2N}} + \phi(x_{2N+1})e^{-ikx_{2N+1}}\right)\\ &= \Delta x\left(\frac{1}{2}\phi(x_1)e^{-ikx_1} + \phi(x_2)e^{-ikx_2}\right.\\ &\qquad \left. +\ldots + \phi(x_{2N})e^{-ikx_{2N}} + \frac{1}{2}\phi(x_{2N+1})e^{-ikx_{2N+1}}\right).\end{aligned}$$

Due to the periodicity of ϕ, we have $\phi(x_1)e^{-ikx_1} = \phi(x_{2N+1})e^{-ikx_{2N+1}}$, so the integral becomes

$$\int_0^{2\pi} \phi(x,t)e^{-ikx}dx \approx \Delta x\left(\phi(x_1)e^{-ikx_1} + \phi(x_2)e^{-ikx_2} + \ldots + \phi(x_{2N})e^{-ikx_{2N}}\right)$$

with the interval $\Delta x = \frac{\pi}{N}$, due to the fact that there are $2N$ collocation points over an interval of 2π, therefore

$$\int_0^{2\pi} \phi(x,t)e^{-ikx}dx \approx \frac{\pi}{N}\left(\phi(x_1)e^{-ikx_1} + \phi(x_2)e^{-ikx_2} + \ldots + \phi(x_{2N})e^{-ikx_{2N}}\right).$$

Substituting this into the expression for the Fourier coefficients in the even case (Eq. (4)) gives

$$\begin{aligned}\hat{\phi}_k(t) &\approx \frac{1}{2\pi}\frac{\pi}{N}\left(\phi(x_1)e^{-ikx_1} + \phi(x_2)e^{-ikx_2} + \ldots + \phi(x_{2N})e^{-ikx_{2N}}\right)\\ &= \frac{1}{2N}\left(\phi(x_1)e^{-ikx_1} + \phi(x_2)e^{-ikx_2} + \ldots + \phi(x_{2N})e^{-ikx_{2N}}\right)\\ &= \frac{1}{2N}\sum_{n=1}^{2N}\phi(x_n)e^{-ikx_n}.\end{aligned} \tag{5}$$

Three pieces of information are necessary before this can be further manipulated. Firstly, the fact that ϕ is an even function implies that $x_{2N+1-n} = 2\pi - x_n$, which, combined by the fact that for even functions $\phi(x) = \phi(2\pi - x)$, yields

$$\phi(x_{2N-n+1}) = \phi(x_n). \tag{6}$$

Secondly, using the Euler identity gives $(e^{i\pi})^2 = (-1)^2$ so $(e^{i2\pi})^k = 1^k$, i.e. $e^{ik2\pi} = 1$ so

$$e^{ik(2\pi - x)} = e^{ik2\pi}e^{-ikx} = e^{-ikx}. \tag{7}$$

Thirdly, from the definition of cosine we have

$$2\cos(x) = e^{ix} + e^{-ix}. \tag{8}$$

Using (6), we can see that $\phi(x_1) = \phi(x_{2N})$, $\phi(x_2) = \phi(x_{2N-1})$, etc. So the series (5) can be rewritten as

$$\begin{aligned}\hat{\phi}_k(t) \approx \frac{1}{2N}\left[\phi(x_1)\left(e^{-ikx_1} + e^{-ikx_{2N}}\right) + \phi(x_2)\left(e^{-ikx_2} + e^{-ikx_{2N-1}}\right)\right. \\ \left. +\ldots + \phi(x_N)\left(e^{-ikx_N} + e^{-ikx_{N+1}}\right)\right].\end{aligned}$$

As already mentioned, because ϕ is even $x_{2N+1-n} = 2\pi - x_n$, i.e. $x_{2N} = 2\pi - x_1$ etc. hence

$$\begin{aligned}\hat{\phi}_k(t) \approx \frac{1}{2N}\left[\phi(x_1)\left(e^{-ikx_1} + e^{-ik(2\pi - x_1)}\right) + \phi(x_2)\left(e^{-ikx_2} + e^{-ik(2\pi - x_2)}\right)\right. \\ \left. +\ldots + \phi(x_N)\left(e^{-ikx_N} + e^{-ik(2\pi - x_N)}\right)\right].\end{aligned}$$

Using (7) and then (8) gives

$$\begin{aligned}\hat{\phi}_k(t) &\approx \frac{1}{2N}\left[\phi(x_1)\left(e^{-ikx_1} + e^{ikx_1}\right) + \phi(x_2)\left(e^{-ikx_2} + e^{ikx_2}\right) + \ldots + \phi(x_N)\left(e^{-ikx_N} + e^{ikx_N}\right)\right] \\ &= \frac{1}{2N}\left[\phi(x_1)2\cos(kx_1) + \phi(x_2)2\cos(kx_2) + \ldots + \phi(x_N)2\cos(kx_N)\right] \\ &= \frac{1}{N}\left[\phi(x_1)\cos(kx_1) + \phi(x_2)\cos(kx_2) + \ldots + \phi(x_N)\cos(kx_N)\right] \\ &= \frac{1}{N}\sum_{n=1}^{N}\phi(x_n)\cos(kx_n). \end{aligned} \tag{9}$$

Henceforth, $\tilde{\phi}_k$ will denote the series approximation to distinguish it from the exact Fourier coefficients $\hat{\phi}_k$. In keeping with a truncation of (2), $\tilde{\phi}_k$ will be computed for N values of k, starting at $k = 0$. Note that the number of collocation points

has been more than halved as j in (3) now ranges from 1 to N and spans $[0, \pi]$. Therefore the Discrete Cosine Transform (DCT) is finally found to be,

$$\tilde{\phi}_k = \frac{1}{N} \sum_{n=1}^{N} \phi(x_n) \cos(kx_n), k = 0, ..., N-1.$$

Consequently, the Inverse Discrete Cosine Transform is given by

$$\phi(x_n) = \sum_{k=0}^{N-1} w(k) \tilde{\phi}_k \cos(kx_n), n = 1, ..., N$$

with weights

$$w(k) = \begin{cases} 1, k = 0 \\ 2, k \geq 1. \end{cases}$$

2.3 Discrete cosine transform in MATLAB

The discrete cosine transform and the inverse discrete cosine transform are inbuilt functions in MATLAB. There are several standard variants of the DCT defined by the function call **dct**. However, the default variant is given here

$$\mathbf{dct}(x) = \sum_{n=1}^{N} v(k) x(n) \cos(kx_n) = y(k)$$
$$\mathbf{idct}(y) = \sum_{k=0}^{N-1} v(k) y(k) \cos(kx_n) = x(n)$$

where

$$v(k) = \begin{cases} \sqrt{\frac{1}{N}}, k = 0 \\ \sqrt{\frac{2}{N}}, k \geq 1. \end{cases} \tag{10}$$

This definition is similar to the definition given above, the only differences arise in the missing factor of $\frac{1}{N}$ and the differences in the weights $w(k)$ and $v(k)$. The two definitions are however equivalent.

In our notation, the MATLAB definitions are

$$\hat{\phi}_k = \sum_{n=1}^{N} v(k)\phi(x_n)\cos(kx_n), k = 0, ..., N-1 \tag{11}$$

$$\phi(x_n) = \sum_{k=0}^{N-1} v(k)\hat{\phi}_k \cos(kx_n), n = 1, ..., N. \tag{12}$$

2.4 Differentiation matrices

One benefit of using cosine collocation to solve partial differential equations is that the derivative of the function can be expressed as a product of a differentiation matrix and the coefficients of the series approximation of the function. Enforcing (12) at the N collocation points (which will be denoted by ϕ_N) and differentiating with respect to x gives that

$$\phi_N'(x_m) = -\sum_{k=0}^{N-1} kv(k)\hat{\phi}_k \sin(kx_m).$$

Substituting (11) we find

$$\phi_N'(x_m) = -\sum_{k=0}^{N-1} kv(k)\left(v(k)\sum_{n=1}^{N}\phi_N(x_n)\cos(kx_n)\right)\sin(kx_m).$$

We can write this in the form of a product of a differentiation matrix and the function coefficients. If the matrix $\mathbf{D_1}$ is defined as

$$\mathbf{D_1}(m,n) = -\sum_{k=0}^{N-1} kv^2(k)\cos(kx_n)\sin(kx_m)$$

then the derivative of ϕ_N can be written as

$$\phi_N'(x_m) = \sum_{n=1}^{N}\mathbf{D_1}(m,n)\phi_N(x_n).$$

A more compact notation is to let $\phi_i = \phi_p(x_i), \phi_i' = \phi_p'(x_i)$ etc and then define the vectors

$$\begin{aligned}
\mathbf{x} &:= (x_1, x_2, ..., x_N) \\
\mathbf{\Phi}_p(\mathbf{x}) &:= (\phi_1, \phi_2, ..., \phi_N) \\
\mathbf{\Phi}_p'(\mathbf{x}) &:= (\phi_1', \phi_2', ..., \phi_N') \\
\mathbf{\Phi}_p''(\mathbf{x}) &:= (\phi_1'', \phi_2'', ..., \phi_N'')
\end{aligned}$$

so we may express the derivatives as products of matrices with vectors

$$\begin{aligned}
\mathbf{\Phi}_p &= \mathbf{D_0}\mathbf{\Phi}_p \\
\mathbf{\Phi}_p' &= \mathbf{D_1}\mathbf{\Phi}_p \\
\mathbf{\Phi}_p'' &= \mathbf{D_2}\mathbf{\Phi}_p.
\end{aligned}$$

Obviously, $\mathbf{D_0}$ is the $N \times N$ identity matrix, and $\mathbf{D_1}$ is as defined above. The matrix $\mathbf{D_2}$ is derived in a similar manner and we find that

$$\phi_N''(x_m) = -\sum_{k=0}^{N-1} k^2 v(k) \left(v(k) \sum_{n=1}^{N} \phi_N(x_n) \cos(kx_n) \right) \cos(kx_m),$$

thus the second differentiation matrix can be written as

$$\mathbf{D_2}(m,n) = -\sum_{k=0}^{N-1} k^2 v^2(k) \cos(kx_n) \cos(kx_m),$$

and the differentiation takes the form

$$\phi_N''(x_m) = \sum_{n=1}^{N} \mathbf{D_2}(m,n) \phi_N(x_n).$$

2.5 Newton's method

Our approach to solving partial differential equations leads, eventually, to solving a set of nonlinear algebraic equations for the coefficients of our function approximation. We use Newton's method for this task (see, for example, Bradie, section 3.10, [3]). The general idea of Newton's method in solving a scalar equation of the form $f(x) = 0$ is to choose an initial guess x_0 such that $f(x_0) \approx 0$, i.e. an initial guess close to the actual solution. Then the x-intercept of the line of the tangent to $y = f(x)$ at $x = x_0$ provides an improved estimate. This procedure is iterated until the required precision is met. This takes the form

$$x_{n+1} = x_n - \frac{f(x_n)}{f'(x_n)}.$$

This approach can be generalised to higher dimensional problems, i.e. a system of nonlinear equations. We wish to solve the problem $\mathbf{F}(\mathbf{x}) = \mathbf{0}$, where $\mathbf{F} : \mathbb{R}^N \to \mathbb{R}^N$, an N-dimensional vector of functions, and $\mathbf{x}$ is a vector of size N. Like the scalar version we start with an initial guess $\mathbf{x}_0$ and then iterate as follows:

$$\mathbf{x}^{n+1} = \mathbf{x}^n - \frac{\mathbf{F}(\mathbf{x}^n)}{\mathbf{F}'(\mathbf{x}^n)}.$$

The derivative of $\mathbf{F}(\mathbf{x})$ is the Jacobian matrix and is denoted by $\mathbf{J}(\mathbf{x})$. Division by a matrix is not defined in general, so we multiply first by the Jacobian and then by the inverse of the Jacobian to find:

$$\mathbf{x}^{n+1} = \mathbf{x}^n - [\mathbf{J}(\mathbf{x}^n)]^{-1}\mathbf{F}(\mathbf{x}^n).$$

We define the vector $\mathbf{v}^n$ to be

$$\mathbf{v}^n := -[\mathbf{J}(\mathbf{x}^n)]^{-1}\mathbf{F}(\mathbf{x}^n)$$

and if we multiply across by the Jacobian we find

$$[\mathbf{J}(\mathbf{x}^{(n)})]\mathbf{v}^{(n)} = -\mathbf{F}(\mathbf{x}^{(n)}). \tag{13}$$

Eq. (13) is a linear system of equations and can be readily solved for $\mathbf{v}^n$, and hence we iterate:

$$\mathbf{x}^{n+1} = \mathbf{x}^n + \mathbf{v}^n.$$

Each iteration of Newton's method for this problem involves solving a linear system of equations.

2.6 Applications

In this section, solutions will be found using the cosine collocation method to the Burgers, KdV, KdV-B, Whitham-B, Whitham, and CV-Whitham equations. While most of the cosine collocation method was derived and detailed above, some examples needed further work, for instance, where a convolution kernel was present. Results are included here for all equations except for the CV-Whitham equation. The results for the CV-Whitham equation are found in Section 4. We delay showing the CV-Whitham results so that the entire process of both solution and stability analysis are reported in one place.

2.6.1 Korteweg-deVries and Burgers equation

The KdV equation in dimensional form is given by

$$\eta_t + c_0\eta_x + \frac{3}{2}\frac{c_0}{h_0}\eta\eta_x + \frac{1}{6}c_0h_0^2\eta_{xxx} = 0$$

where h_0 is the undisturbed height of the water surface and c_0 is the phase speed. The scalings [26]

$$x \mapsto h_0 x, \quad t \mapsto \frac{h_0}{c_0} t, \quad \eta \mapsto \frac{2}{3} h_0 \eta$$

give the nondimensional KdV equation

$$\eta_t + \eta_x + \eta\eta_x + \delta\eta_{xxx} = 0, \text{ where } \delta = \frac{1}{6}.$$

The Burger's equation in its general form is given by

$$\eta_t + \eta\eta_x = \epsilon\eta_{xx},$$

where ϵ dictates the strength of the diffusion term.

Combining the second derivative dispersion term from the Burger's equation with the nondimensional KdV equation yields the Korteweg-deVries-Burgers (KdV-B) equation:

$$\eta_t + \eta_x + \eta\eta_x + \delta\eta_{xxx} = \epsilon\eta_{xx}.$$

The travelling wave ansatz $\eta(x,t) = \phi(x - ct)$ is used to get

$$-c\phi' + \phi' + \phi\phi' + \delta\phi''' - \epsilon\phi'' = 0$$
$$(-c+1)\phi' + \phi\phi' + \delta\phi''' - \epsilon\phi'' = 0.$$

Integrating this, which involves undoing the chain rule on the nonlinear term, gives

$$(-c+1)\phi + \frac{1}{2}\phi^2 + \delta\phi'' - \epsilon\phi' = 0.$$

Further details can be found in Appendix 7.2, which highlights the pertinent details of the work of Bona and Schonbek [1], including the permissibility of the constant of integration being zero. We change the domain of this equation from $[0, L]$ to $[0, \pi]$ for the sake of simplicity in applying the cosine collocation method. For this the

scaling

$$\phi(x) \mapsto \phi(ax) \text{ with } a = \frac{L}{\pi}$$

is used, which gives

$$(-c+1)\phi + \frac{1}{2}\phi^2 + \delta a^{-2}\phi'' - \epsilon a^{-1}\phi' = 0, 0 \leq x \leq \pi.$$

At this point, the actual cosine collocation can start, as we use the differentiation matrices derived above and enforce ϕ at the N collocation points to give

$$(-c+1)\phi_N + \frac{1}{2}\phi_N^2 + \delta a^{-2}\mathbf{D_2}\phi_N - \epsilon a^{-1}\mathbf{D_1}\phi_N = 0.$$

Note that ϕ_N is the vector $(\phi(x_1), \phi(x_2), ..., \phi(x_N))$, i.e. $\phi(x)$ at each of the N x-coordinates, ϕ_N^2 is an element-wise product of this vector, and products of the differentiation matrices $\mathbf{D_1}$ and $\mathbf{D_2}$ and the vector ϕ_N are dot products. This means the PDE has now been reduced to a system of N coupled, nonlinear, algebraic equations. This system of equations can be solved using Newton's method. For this, we need the Jacobian of the mapping $\mathbf{F} : \phi_N \mapsto (-c+1)\phi_N + \frac{1}{2}\phi_N^2 + \delta a^{-2}\mathbf{D_2}\phi_N - \epsilon a^{-1}\mathbf{D_1}\phi_N$. The Jacobian of $\mathbf{F}$ is

$$\mathscr{J}(\mathbf{F}) = (-c+1)\mathbf{I} + \text{diag}(\phi_N) + \delta a^{-2}\mathbf{D_2} - \epsilon a^{-1}\mathbf{D_1},$$

where $\mathbf{I}$ is the identity matrix, and $\text{diag}(\phi_N)$ is notation borrowed from MATLAB, denoting a square diagonal matrix with the elements of the vector ϕ_N on the main diagonal.

Note that the coefficient of the second derivative term is ϵ and the coefficient of the third derivative term has been defined as δ. While in the KdV equation $\delta = \frac{1}{6}$, defining this as a parameter δ allows generic code to be written for the complete KdV-B equation, with the option to "switch off" the Burgers term (i.e. set $\epsilon = 0$) when one wants to look at the standard KdV equation, or alternatively "switch-off" the third derivative dispersion term (i.e. set $\delta = 0$) to find solutions of the Burgers

equation. When both ϵ and δ are non-zero the complete KdV-B equation is under consideration. Solutions were found to all of these; example plots are shown below.

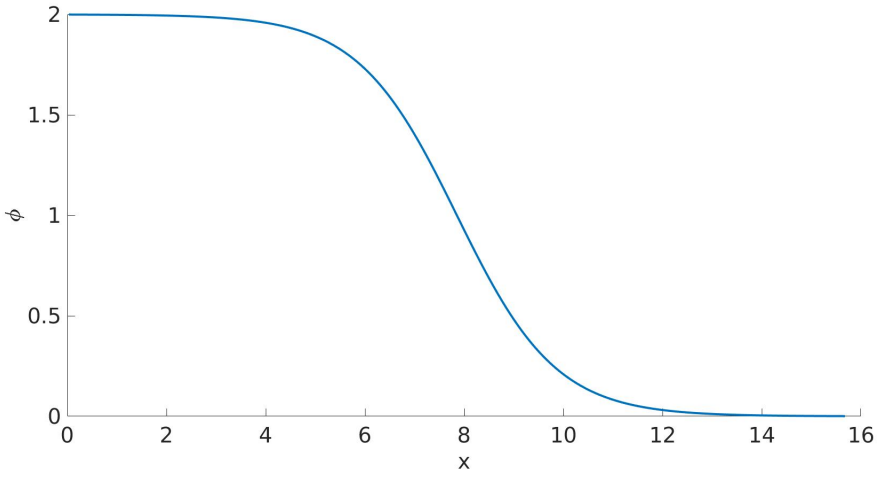
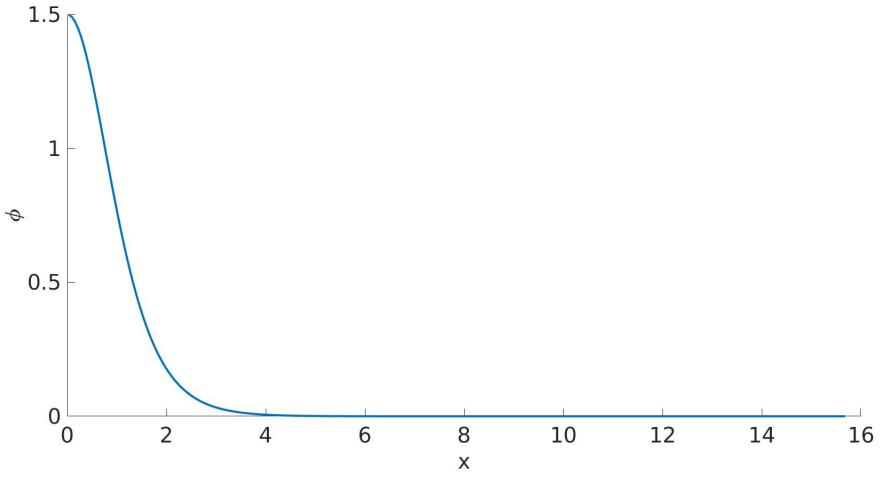


Figure 1: Solution to the Burgers equation with wave speed $c = 2$.

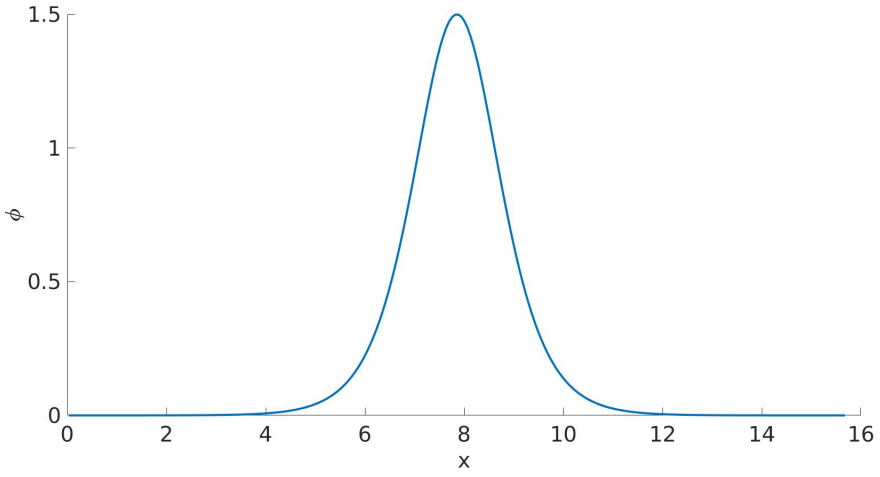
Figure 1 depicts a solution for the Burgers equation for wave speed $c = 2$, with scaling $a = 5$. To find solutions, Newton's method requires an initial guess that is sufficiently close to the sought solution. Nevland [26] used the exact solution to the Burgers equation from Bona and Schonbek [1] as a guide and therefrom used tanh-waves as initial guesses for the Burgers equation. The solution in Figure 1 was found with the initial guess $\phi = \tanh(2(x - \frac{\pi}{2}))$ and is the same as that given by Nevland, which gives us confidence that the code works well. This solution could be mirrored and plotted on a greater domain due to its evenness and periodicity.

Figure 2 depicts two solutions to the KdV equation, with wave speed $c = 1.5$ and scaling $a = 5$. The difference between Figure 2a and 2b is the use of different initial guesses. In Figure 2a, the initial guess was $\phi = \text{sech}^2(2x)$, whilst in Figure 2b the initial guess was $\phi = \text{sech}^2(x)$. Nevland found that if the crest of the wave of the initial guess was close to zero, it tended to converge towards the first solution, whereas, for initial guesses where the crest was away from zero, it tended to converge to the second. This is consistent with our results.

Figure 3 depicts two solutions to the KdV-B equation. Recall that for the KdV-



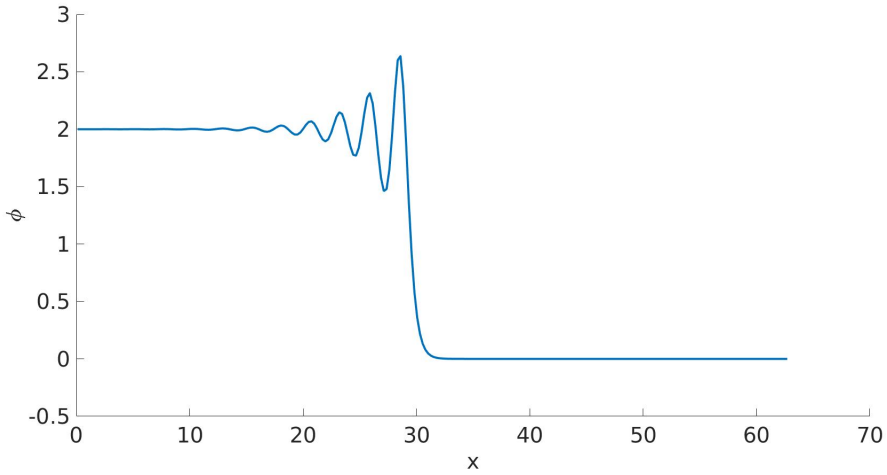
(a) Initial guess $\phi = \text{sech}^2(2x)$



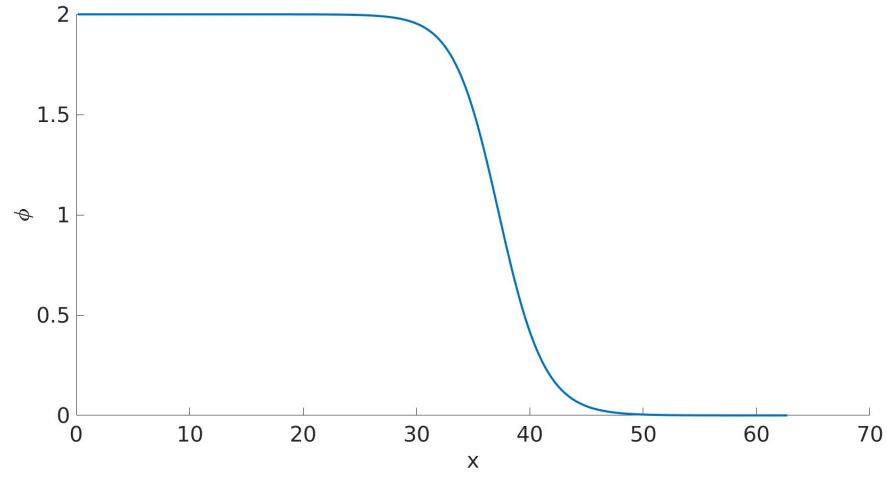
(b) Initial guess $\phi = \text{sech}^2(x)$

Figure 2: Solutions to the KdV equation with wave speed $c = 1.5$ with differing initial guesses applied.

B equation, both the third derivative dispersive term originating from the KdV equation and the second derivative dispersive term originating from the Burgers equation are included. The strength of these terms is determined by coefficients δ and ϵ respectively. In both the solutions given in Figure 3, $\delta = 1$, the wave speed is $c = 2$, the scaling is $a = 20$, and the initial guess is $\phi = 1 - \tanh(3(x - \frac{\pi}{2}))$. The difference between them is that the solution in Figure 3a is to the KdV-B equation with $\epsilon = 0.1$, while Figure 3b is for $\epsilon = 2$. As Nevland states, the former gives a solution resembling an undular bore, while the latter resembles a tanh-wave, which



(a) $\epsilon = 0.1$



(b) $\epsilon = 2$

Figure 3: Solutions to the KdV-B equation with wave speed $c = 2$, and initial guess $\phi = 1 - \tanh(3(x - \frac{\pi}{2}))$.

is consistent with the results proven by Bona and Schonbek [1]. These too could be mirrored and plotted on a larger domain due to their evenness and periodicity, and such results can be seen in Nevland's work [26].

2.6.2 Whitham-Burgers equation

The Whitham equation is similar to the KdV equation, except that the dispersion term, i.e. the third derivative, is replaced with a kernel which takes the form of a

Fourier multiplier. By including a Burgers term the Whitham equation becomes the Whitham-Burgers equation in the same way it was included in the KdV equation to give the KdV-B equation.

The dimensional Whitham equation is given by

$$\eta_t + \frac{3}{2}\frac{c_0}{h_0}\eta\eta_x + K_{h_0} * \eta_x = 0$$

where the kernel K_{h_0} is the Fourier multiplier defined by

$$\hat{K}_{h_0} = \mathcal{F}\{K_{h_0}\} = \sqrt{\frac{g\tanh(kh_0)}{k}}$$

or equivalently

$$K_{h_0} = \mathcal{F}^{-1}\left\{\sqrt{\frac{g\tanh(kh_0)}{k}}\right\}.$$

Using the same scalings as above (see Section 2.6.1), noting that $c_0 = \sqrt{gh_0}$ [26],

$$x \mapsto h_0 x, \quad t \mapsto \frac{h_0}{c_0}t, \quad \eta \mapsto \frac{2}{3}h_0\eta$$

the non dimensional Whitham equation becomes

$$\eta_t + \eta\eta_x + K * \eta_x = 0$$

and the convolution term is scaled by

$$K_{h_0} * \eta_x \mapsto \frac{2}{3}c_0(K * \eta_x)$$

so that the kernel K becomes

$$K = \mathcal{F}^{-1}\left\{\sqrt{\frac{\tanh(k)}{k}}\right\}. \tag{14}$$

This change to the dispersion term aimed to address the shortcoming of the KdV equation, in that the KdV only models the linear phase velocity of the water-wave

problem for the shallow water / long wave limit [6]. This choice of kernel incorporates both full linear dispersion with long wave nonlinearity [31], and hence models the one-directional phase velocity of the full water-wave problem [6].

Bringing in the Burgers term, we have that the Whitham-Burgers equation is

$$\eta_t + \eta\eta_x + K * \eta_x = \epsilon\eta_{xx}$$

with the kernel K given in Eq. (14).

The travelling wave ansatz $\eta(x,t) = \phi(x - ct)$ is applied giving

$$-c\phi' + \frac{1}{2}(\phi^2)' + K * \phi' - \epsilon\phi'' = 0$$

which is integrated (see Appendix 7.2 or [1] for details) to give

$$-c\phi + \frac{1}{2}\phi^2 + K * \phi - \epsilon\phi' = 0.$$

To change the domain from $[0, L]$ to $[0, \pi]$ we scale by

$$\phi(x) \mapsto \phi(ax) \text{ with } a = \frac{L}{\pi}$$

to give

$$-c\phi + \frac{1}{2}\phi^2 + \sqrt{a}K_{\frac{1}{a}} * \phi - \epsilon a^{-1}\phi' = 0, 0 \leq x \leq \pi \tag{15}$$

where $K_{\frac{1}{a}} = \mathcal{F}^{-1}\left(\sqrt{\frac{\tanh(\frac{k}{a})}{k}}\right)$.

Previously, when we were solving the KdV-B equation by cosine collocation, we used the matrices $\mathbf{D_1}$ and $\mathbf{D_2}$; in this case, we will continue to use the $\mathbf{D_1}$ term for the Burgers term, but a different matrix will be required to represent the convolution product.

It can be shown [26] that

$$K_{\frac{1}{a}} * \phi_N = \sum_{k=0}^{N-1} v(k)\hat{K}_{\frac{1}{a}}(k)\tilde{\phi}_k \cos(kx)$$

and as such, we can write the following, where a substitution of (11) is used again

$$\begin{aligned}(K_{\frac{1}{a}} * \phi_N)(x_m) &= \sum_{k=0}^{N-1} v(k)\hat{K}_{\frac{1}{a}}(k)\tilde{\phi}_k \cos(kx_m) \\ &= \sum_{k=0}^{N-1} v(k)\hat{K}_{\frac{1}{a}}(k) \left[v(k) \sum_{n=1}^{N} \phi_N(x_n)\cos(kx_n) \right] \cos(kx_m) \\ &= \sum_{n=1}^{N} \underbrace{\left[\sum_{k=0}^{N-1} v^2(k)\hat{K}_{\frac{1}{a}}(k)\cos(kx_n)\cos(kx_m) \right]}_{\text{A}} \phi_N(x_n).\end{aligned}$$

Looking more closely at the contents of the square brackets (labelled A) with a view to inserting the kernel, shows

$$\begin{aligned}&\sum_{k=0}^{N-1} v^2(k)\hat{K}_{\frac{1}{a}}(k)\cos(kx_n)\cos(kx_m) = \\ &\qquad v^2(0)\hat{K}_{\frac{1}{a}}(0)\cos(0)\cos(0) + \sum_{k=1}^{N-1} v^2(k)\hat{K}_{\frac{1}{a}}(k)\cos(kx_n)\cos(kx_m).\end{aligned}$$

The term $\hat{K}_{\frac{1}{a}}(0)$ appears to involve dividing by 0 but taking the limit

$$\hat{K}_{\frac{1}{a}}(0) = \lim_{k\to 0} \sqrt{\frac{\tanh(\frac{k}{a})}{k}} = \frac{1}{\sqrt{a}}$$

which, recalling the definitions of v from (10), gives

$$\sum_{k=0}^{N-1} v^2(k)\hat{K}_{\frac{1}{a}}(k)\cos(kx_n)\cos(kx_m) = \frac{1}{N\sqrt{a}} + \sum_{k=1}^{N-1} \frac{2}{N}\sqrt{\frac{\tanh(\frac{k}{a})}{k}}\cos(kx_n)\cos(kx_m).$$

To summarise, this means the entire convolution product can be written as

$$(K_{\frac{1}{a}} * \phi_N)(x_m) = \sum_{n=1}^{N} \mathbf{K}^{\mathbf{N}}_{\frac{\mathbf{1}}{\mathbf{a}}}(m,n)\phi_N(x_n)$$

where the matrix $\mathbf{K}^{\mathbf{N}}_{\frac{\mathbf{1}}{\mathbf{a}}}(m,n)$ is

$$\mathbf{K}^{\mathbf{N}}_{\frac{\mathbf{1}}{\mathbf{a}}}(m,n) = \frac{1}{N\sqrt{a}} + \sum_{k=1}^{N-1} \frac{2}{N}\sqrt{\frac{\tanh(\frac{k}{a})}{k}}\cos(kx_n)\cos(kx_m). \tag{16}$$

Therefore, when we apply cosine collocation with the first derivative matrix and the convolution product matrix to (15), we get the system of equations

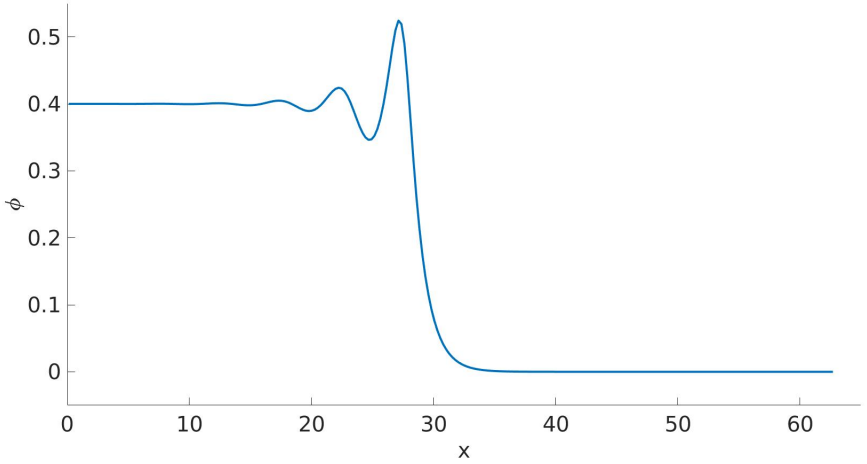
$$-c\phi_N + \frac{1}{2}\phi_N^2 + \sqrt{a}\mathbf{K}^{\mathbf{N}}_{\frac{\mathbf{1}}{\mathbf{a}}}\phi_N - \epsilon a^{-1}\mathbf{D_1}\phi_N = 0,$$

where $\phi_N = (\phi_N(x_1), ..., \phi_N(x_N))^T$.

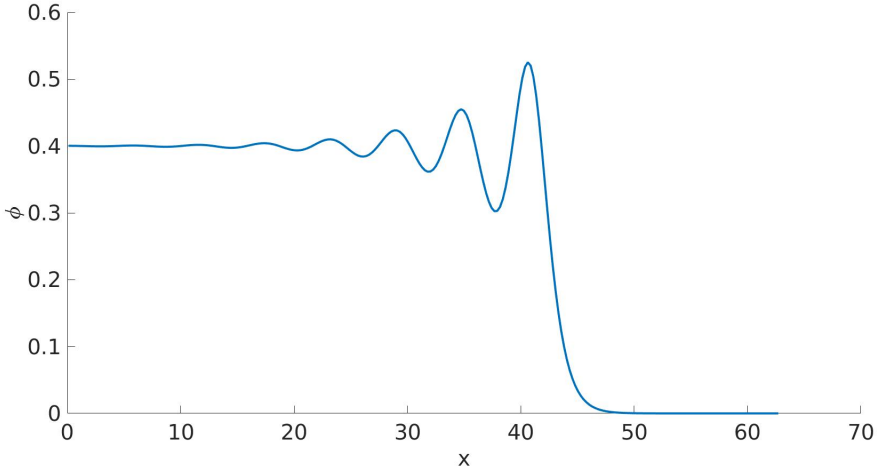
To solve using Newton's method, the Jacobian of the mapping $\mathbf{F} : \phi_N \mapsto -c\phi_N + \frac{1}{2}\phi_N^2 + \sqrt{a}\mathbf{K}^{\mathbf{N}}_{\frac{\mathbf{1}}{\mathbf{a}}}\phi_N - \epsilon a^{-1}\mathbf{D_1}\phi_N$ is needed. The Jacobian of $\mathbf{F}$ is

$$\mathscr{J}(\mathbf{F}) = -c\mathbf{D_0} + \mathrm{diag}(\phi_N) + \sqrt{a}\mathbf{K}^{\mathbf{N}}_{\frac{\mathbf{1}}{\mathbf{a}}} - \epsilon a^{-1}\mathbf{D_1}.$$

Figure 4a depicts a solution to the Whitham-Burgers equation for wave speed $c = 1.2$, scaling $a = 20$, with the coefficient of the Burgers term $\epsilon = 0.05$. It is much akin to the undular bore solutions for the KdV-B equation, with slightly weaker dispersions. For comparison, Figure 4b shows the solution to the KdV-B equation with $\delta = 1$ and the same values of c, a, and ϵ as Figure 4a. Nevland [26] states that the stronger dispersions evident in the figures of the KdV-B solutions are logical, given that the dispersive term in the KdV-B equation is stronger than that of the Whitham-B equation. The initial guesses required to achieve these solutions also differed, which is not unexpected for different equations, and were $\phi = 0.2(1 - \tanh(6(x - \frac{\pi}{2})))$ and $\phi = 1 - \tanh(3(x - \frac{\pi}{2}))$, for the Whitham-Burgers



(a) Whitham-Burgers equation



(b) KdV-B equation

Figure 4: Solutions to the Whitham-B and KdV-B equations with $c = 1.2$ and $\epsilon = 0.05$.

and KdV-B equations respectively.

2.6.3 Whitham equation

Sanford et al. [28] analysed a very similar Whitham equation, which only differs from the example above in that it doesn't contain a Burgers term. It is given in the form

$$\eta_t + \frac{3}{2}\eta\eta_x + K * \eta_x = 0$$

where again

$$\hat{K}(k) = \sqrt{\frac{\tanh(k)}{k}}.$$

This is scaled using $\eta \mapsto \frac{3}{4}\eta$ to give

$$\eta_t + 2\eta\eta_x + K * \eta_x = 0,$$

and the same $\hat{K}$. Applying the travelling wave ansatz $\eta(x,t) = \phi(x - ct)$ and integrating gives

$$-c\phi + \phi^2 + K * \phi = 0.$$

This can be rescaled as above using

$$\phi(x) = \phi(ax) \text{ with } a = \frac{L}{\pi}$$

to again redefine it to the domain $[0, \pi]$, giving

$$-c\phi + \phi^2 + \sqrt{a}K * \phi = 0$$

and

$$\hat{K}_{\frac{1}{a}}(k) = \sqrt{\frac{\tanh(\frac{k}{a})}{k}}.$$

Enforcing this at the collocation points and taking the same convolution kernel matrix as for the Whitham-Burgers equation (as the definitions of $\hat{K_{\frac{1}{a}}}$ are the same), we have the mapping

$$\mathbf{F} : \phi_n \mapsto -c\phi_N + \phi_n^2 + \sqrt{a}\mathbf{K}^{\mathbf{N}}_{\frac{\mathbf{1}}{\mathbf{a}}}\phi_N$$

with the corresponding Jacobian

$$\mathscr{J}(\mathbf{F}) = -c\mathbf{D_0} + 2\text{diag}(\phi_N) + \sqrt{a}\mathbf{K}^{\mathbf{N}}_{\frac{\mathbf{1}}{\mathbf{a}}}.$$

This is the same as the Whitham-Burgers equation with the simple change of a coefficient and the absence of the Burgers term.

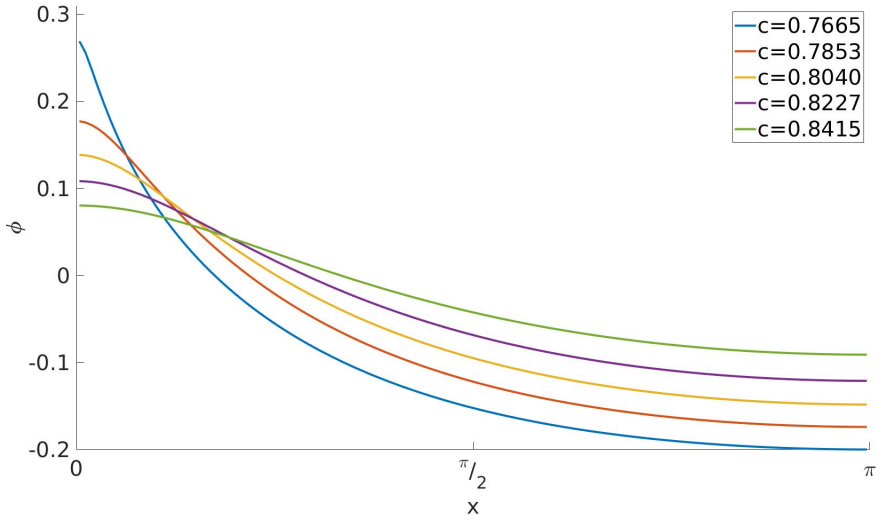


Figure 5: Solutions to the Whitham equation for varying values of c and continually updating initial guesses.

The solutions found for this are depicted in Figure 5. In this case, the initial guess $\phi = 0.3\,\mathrm{sech}^2(x) - 0.15$ was used to find the solution when $c = 0.7665$; c was then incremented and, for each new value of c, the initial guess was the solution found for the previous value of c. Carter et al. used this method of continually updating the initial guess in [6]. The results given in Figure 5 match those found by Sanford et al. [28]. For higher values of the wave speed c, the wave height of the solution is lower, and the solution is less steep, similar to cnoidal solutions of the KdV equation [28]. For low values of c, the solutions have greater wave height and steepness, unlike the KdV equation. Note that, as these are specifically even solutions, an assumption of the cosine collocation method, they are symmetric about $x = 0$ and Sanford et al. [28] show them for x in the domain $(-\pi, \pi)$.

2.6.4 Cubic-Vortical Whitham equation

The same steps are repeated for the Cubic-Vortical Whitham equation as described by Carter et al. [6]. The equation is

$$\eta_t + \mathcal{K} * \eta_x + \alpha\eta\eta_x + \beta\eta^2\eta_x = 0,$$

where

$$\hat{\mathcal{K}}(k) = -\frac{\Omega \tanh(k)}{2k} + \sqrt{\frac{\tanh(k)}{k} + \frac{\Omega^2 \tanh^2(k)}{4k^2}} \tag{17}$$

and

$$\alpha = \frac{\Omega^2 + 3}{\sqrt{\Omega^2 + 4}},$$
$$\beta = -\frac{6 + \Omega^2}{2(4 + \Omega^2)^{\frac{3}{2}}},$$

where Ω is the opposite sign of the constant vorticity. Using the travelling wave ansatz $\eta(x,t) = \phi(x - ct)$ and integrating gives

$$-c\phi + \mathcal{K} * \phi + \frac{\alpha}{2}\phi^2 + \frac{\beta}{3}\phi^3 = 0. \tag{18}$$

We now wish to enforce this at the collocation points. However, as the kernel is defined differently, the convolution kernel matrix is also different and the matrix defined in (16) is no longer valid. However, we have that

$$\mathcal{K} * \phi_N = \sum_{k=0}^{N-1} v(k)\hat{\mathcal{K}}(k)\tilde{\phi}_k \cos(kx)$$

so that by substituting in Eq. (11)

$$\begin{aligned}(\mathcal{K} * \phi_N)(x_m) &= \sum_{k=0}^{N-1} v(k)\hat{\mathcal{K}}(k)\tilde{\phi}_k \cos(kx_m) \\ &= \sum_{k=0}^{N-1} v(k)\hat{\mathcal{K}}(k) \left[v(k) \sum_{n=1}^{N} \phi_N(x_n)\cos(kx_n) \right] \cos kx_m \\ &= \sum_{n=1}^{N} \underbrace{\left[\sum_{k=0}^{N-1} v^2(k)\hat{\mathcal{K}}(k)\cos(kx_n)\cos(kx_m) \right]}_{\text{A}} \phi_N(x_n).\end{aligned}$$

The contents of the square brackets (labelled A) can be written as

$$\begin{aligned}&\sum_{k=0}^{N-1} v^2(k)\hat{\mathcal{K}}(k)\cos(kx_n)\cos(kx_m) = \\ &\qquad v^2(0)\hat{\mathcal{K}}(0)\cos(0)\cos(0) + \sum_{k=1}^{N-1} v^2(k)\hat{\mathcal{K}}(k)\cos(kx_n)\cos(kx_m).\end{aligned}$$

So far, this is the same derivation as given above for (16). The change occurs now when we substitute in (17). The zero case $\hat{\mathcal{K}}(0)$ would involve dividing by 0, so we take the limit

$$\lim_{k\to 0} \hat{\mathcal{K}}(k) = \frac{1}{2}\left(-\Omega + \sqrt{4+\Omega^2}\right)$$

which, in addition to substituting for $v(k)$ as defined in (10), gives that

$$\begin{aligned}&\sum_{k=0}^{N-1} v^2(k)\hat{\mathcal{K}}(k)\cos(kx_n)\cos(kx_m) = \frac{1}{2N}\left(-\Omega + \sqrt{4+\Omega^2}\right) + \\ &\quad \sum_{k=1}^{N-1} \frac{2}{N}\left(-\frac{\Omega\tanh(k)}{2k} + \sqrt{\frac{\tanh(k)}{k} + \frac{\Omega^2\tanh^2(k)}{4k^2}} \right) \cos(kx_n)\cos(kx_m).\end{aligned}$$

This means, the entire convolution product can be written in matrix form as

$$(\mathcal{K} * \phi_N)(x_m) = \sum_{n=1}^{N} \mathbf{K^N}(m,n)\phi_N(x_n),$$

where the matrix $\mathbf{K^N}(m,n)$ is given by

$$\begin{aligned}\mathbf{K^N}(m,n) =& \frac{1}{2N}\left(-\Omega+\sqrt{4+\Omega^2}\right)+\\ &\sum_{k=1}^{N-1}\frac{2}{N}\left(-\frac{\Omega\tanh(k)}{2k}+\sqrt{\frac{\tanh(k)}{k}+\frac{\Omega^2\tanh^2(k)}{4k^2}}\right)\cos(kx_n)\cos(kx_m).\end{aligned}$$

So enforcing (18) at the collocation points, we have the mapping

$$\mathbf{F}:\phi_N\mapsto -c\phi_N+\frac{\alpha}{2}\phi_N^2+\frac{\beta}{3}\phi_N^3+\mathbf{K^N}\phi_N,$$

with its associated Jacobian

$$\mathscr{J}(\mathbf{F})=-c\mathbf{D_0}+\mathrm{diag}(\alpha\phi_N)+\mathrm{diag}(\beta\phi_N^2)+\mathbf{K^N}.$$

Note that all results for the CV-Whitham equation are included in Section 4, where the solutions and their stability will be discussed.

2.7 Alternative Fourier solution method

This solution method differs slightly from the cosine collocation method above and yields the same results. The method is only applied to the CV-Whitham equation and follows a derivation from Carter et al. [6]. However, adapting it to any of the other equations studied is straightforward.

Again considering travelling wave solutions of the form $\eta(x,t)=f(x-ct)$ and integrating gives, as above in Eq. (18)

$$-cf+\mathcal{K}*f+\frac{\alpha}{2}f^2+\frac{\beta}{3}f^3=B,$$

where $c\in\mathbb{R}$ is a constant and f is a smooth, real-valued function of $z=x-ct$ with period L. (In this case, f has been used over ϕ to keep the two solution methods

distinct from one another for legibility; the two are equivalent though.) As above, assume the mean of the solution is 0, despite the fact that this is not invariant as it is in the Whitham case. The Fourier expansion of f

$$f(z) = \sum_{k=-N}^{N} \hat{f}(k) e^{\frac{2\pi i k z}{L}} \tag{19}$$

is substituted in. Assuming the solutions are real and therefore all $\hat{f}$ are real-valued, and additionally, assuming that the solutions are even and therefore $\hat{f}(-k) = \hat{f}(k)$ for $k = 1, ..., N$, gives that

$$\begin{aligned} -c\left(\sum_{k=-N}^{N} \hat{f}(k) e^{\frac{2\pi i k z}{L}}\right) + \mathcal{K}\left(\frac{2\pi k}{L}\right)\left(\sum_{k=-N}^{N} \hat{f}(k) e^{\frac{2\pi i k z}{L}}\right) \\ + \frac{\alpha}{2}\underbrace{\left(\sum_{k=-N}^{N} \hat{f}(k) e^{\frac{2\pi i k z}{L}}\right)^2}_{\text{Square term}} + \frac{\beta}{3}\underbrace{\left(\sum_{k=-N}^{N} \hat{f}(k) e^{\frac{2\pi i k z}{L}}\right)^3}_{\text{Cubic term}} = 0 \end{aligned} \tag{20}$$

for all $k = 1, ..., N$. To ensure the solutions have zero mean, impose $\hat{f}(0) = 0$. The $k = 0$ case determines the integration constant B; otherwise, $\hat{f}(0) = 0$ makes it irrelevant. The square and cubic terms underscored above will now be examined individually, as Fourier convolution is required to expand those powers. The first of them can be written as

$$\left(\sum_{k=-N}^{N} \hat{f}(k) e^{\frac{2\pi i k z}{L}}\right)^2 = \left(\sum_{k'=-N}^{N} \hat{f}(k') e^{\frac{2\pi i k' z}{L}}\right)\left(\sum_{k''=-N}^{N} \hat{f}(k'') e^{\frac{2\pi i k'' z}{L}}\right).$$

Note that the k in one sum is not the same as the k in the other sum, and for that reason, they have been marked as k' and k''. Combining these gives

$$\left(\sum_{k=-N}^{N} \hat{f}(k) e^{\frac{2\pi i k z}{L}}\right)^2 = \sum_{k'} \sum_{k''} \hat{f}(k') \hat{f}(k'') e^{\frac{2\pi i z (k' + k'')}{L}}.$$

Renaming $k' + k'' = k$ and substituting this into the power of e, as well as noting

that $k'' = k - k'$ yields that

$$\left(\sum_{k=-N}^{N} \hat{f}(k) e^{\frac{2\pi i k z}{L}}\right)^2 = \sum_{k'} \sum_{k} \hat{f}(k') \hat{f}(k - k') e^{\frac{2\pi i z k}{L}}.$$

Renaming k' to l for legibility ultimately gives

$$\left(\sum_{k=-N}^{N} \hat{f}(k) e^{\frac{2\pi i k z}{L}}\right)^2 = \sum_{l} \sum_{k} \hat{f}(l) \hat{f}(k - l) e^{\frac{2\pi i z k}{L}}.$$

Starting similarly for the cubic term gives

$$\left(\sum_{k=-N}^{N} \hat{f}(k)\ e^{\frac{2\pi i k z}{L}}\right)^3 = \left(\sum_{k'=-N}^{N} \hat{f}(k') e^{\frac{2\pi i k' z}{L}}\right) \left(\sum_{k''=-N}^{N} \hat{f}(k'') e^{\frac{2\pi i k'' z}{L}}\right) \left(\sum_{k'''=-N}^{N} \hat{f}(k''') e^{\frac{2\pi i k''' z}{L}}\right).$$

Using the result from the square term for the first two brackets, and proceeding similarly, it can be written as

$$\begin{aligned}\left(\sum_{k=-N}^{N} \hat{f}(k) e^{\frac{2\pi i k z}{L}}\right)^3 &= \left(\sum_{l} \sum_{j} \hat{f}(l) \hat{f}(j - l) e^{\frac{2\pi i z j}{L}}\right) \left(\sum_{k'''=-N}^{N} \hat{f}(k''') e^{\frac{2\pi i k''' z}{L}}\right) \\ &= \sum_{k'''} \sum_{l} \sum_{j} \hat{f}(k''') \hat{f}(l) \hat{f}(j - l) e^{\frac{2\pi i z k'''}{L}} e^{\frac{2\pi i z j}{L}} \\ &= \sum_{k'''} \sum_{l} \sum_{j} \hat{f}(k''') \hat{f}(l) \hat{f}(j - l) e^{\frac{2\pi i z (k''' + j)}{L}}.\end{aligned}$$

This time defining that $j + k''' = k$, therefore $k''' = k - j$ and

$$\left(\sum_{k=-N}^{N} \hat{f}(k) e^{\frac{2\pi i k z}{L}}\right)^3 = \sum_{k} \sum_{l} \sum_{j} \hat{f}(k - j) \hat{f}(l) \hat{f}(j - l) e^{\frac{2\pi i z (k)}{L}}.$$

Substituting these results into Eq. (20) yields

$$-c\left(\sum_k \hat{f}(k)e^{\frac{2\pi ikz}{L}}\right)+\mathcal{K}\left(\frac{2\pi k}{L}\right)\left(\sum_k \hat{f}(k)e^{\frac{2\pi ikz}{L}}\right)+\frac{\alpha}{2}\left(\sum_l\sum_k \hat{f}(l)\hat{f}(k-l)e^{\frac{2\pi izk}{L}}\right)$$
$$+\frac{\beta}{3}\left(\sum_k\sum_l\sum_j \hat{f}(k-j)\hat{f}(l)\hat{f}(j-l)e^{\frac{2\pi iz(k)}{L}}\right)=0,\ \forall\ k=1,...,N.$$

Simplifying gives

$$-c\hat{f}(k)+\mathcal{K}\left(\frac{2\pi k}{L}\right)\hat{f}(k)+\frac{\alpha}{2}\left(\sum_l \hat{f}(l)\hat{f}(k-l)\right)$$
$$+\frac{\beta}{3}\left(\sum_l\sum_j \hat{f}(k-j)\hat{f}(l)\hat{f}(j-l)\right)=0\ \forall\ k=1,...,N. \tag{21}$$

Mathematically, the Fourier expansion of f, i.e. $\hat{f}$, is a bi-infinite vector, with k ranging from minus infinity to infinity. However, practically, this cannot be the case in the code, therefore the vector $\hat{f}$ was truncated at a certain size, to be indexed from $-N$ to N, with the central element being the zeroth. In (21), some indices of $\hat{f}$ include $k-l$, $k-j$, and $j-l$. If k, l, and j range from $-N$ to N, these indices would range from $-2N$ to $2N$. Some of these exceed the range of $\hat{f}$ and are therefore invalid. For this reason, the range of the summations must be altered, and are given by Carter et al. [6] as

$$-c\hat{f}(k)+\mathcal{K}\left(\frac{2\pi k}{L}\right)\hat{f}(k)+\frac{\alpha}{2}\left(\sum_{l=\max(-N,-N+k)}^{\min(N,N+k)} \hat{f}(l)\hat{f}(k-l)\right)$$
$$+\frac{\beta}{3}\left(\sum_{l=\max(-N,-N+j)}^{\min(N,N+j)}\ \sum_{j=\max(-2N,-N+k)}^{\min(2N,N+k)} \hat{f}(k-j)\hat{f}(l)\hat{f}(j-l)\right)=0\ \forall\ k=1,...,N.$$

With an appropriate initial guess, this system of equations can then be solved using Newton's method. Note that all results for the CV-Whitham equation are included in Section 4 where the solutions and their stability will be discussed.

3 Spectral stability of solutions - Fourier-Floquet-Hill method

3.1 Fourier-Floquet-Hill method

The method used to determine the spectral stability of the solutions for the equations studied here is the Fourier-Floquet-Hill method (FFHM). This method requires the use of Fourier analysis, followed by the Floquet theorem, hence the name. The addition of "Hill" is a tribute to his development of this technique, which is also sometimes simply referred to as "Hill's method." He originally used this technique, with some adjustments, in 1877. Despite the fact that Hill's use of his method included some crass approximations, it was still surprisingly accurate [10]. He developed the method to analyse the spectrum of what is now known as Hill's equation. Hill developed his equation to study lunar stability [14], but it has had other applications and is used in the areas of mass spectroscopy [29], quantum mechanics [7], quantum optics [13], accelerator physics [23], and electromagnetic structures that are periodic in time [21] and/or space [4].

Before we use the FFHM to determine spectral stability, we must first establish what we mean by that. Spectral stability is defined as follows by Deconinck and Kutz [10].

Definition 3.1 *An equilibrium solution $U(x)$ of a dynamical system $\dot{u} = X(u)$ is* ***spectrally stable*** *if the spectrum of the linear operator obtained by linearising $X(u)$ around $U(x)$ has strictly no positive real part.*

Consider a system $\dot{u} = X(u)$ for a function $u = u(x,t)$, where x is a spatial variable and $\dot{u}$ denotes differentiation of u with respect to time t, indicated by the "dot". In general u can depend on more than one spatial variable in addition to x, however, for simplicity of exposition, we consider only one spatial dimension. X can

be thought of as an operator acting on the function u, the spatial variable x, and its derivatives. The dynamical system can then be written more explicitly as

$$\dot{u} = N(x, u, u_x, u_{xx}, ...).$$

Equilibrium solutions are those solutions u which satisfy $\dot{u} = 0$ [10].

To examine the stability of this system, we consider equilibrium solutions along with a small perturbation

$$u_{\text{pert}}(z, \tau) = u(z) + \epsilon v(z, \tau) + O(\epsilon^2),$$

where $u(z)$ is the equilibrium solution, $v(z, \tau)$ is a real-valued function termed the perturbation, and ϵ is a small positive constant [6]. Note that the notation $u(z)$ and the variable τ are utilised in place of $u(x, t)$, this is in anticipation of a change of variables required to convert the frame of reference to that of the wave speed. In this way travelling wave solutions can be considered as stationary solutions [28]. Accounting for this change of notation here, should make it clearer to read and understand the complete derivation given below.

Substituting the perturbed solution into the dynamical system, linearising, and simplifying gives

$$\dot{v} = \mathcal{L}[u(z)]v + O(\epsilon), \tag{22}$$

where $\mathcal{L}$ is a nonlocal linear differential operator [6].

Because $\mathcal{L}$ is linear and independent of τ, it can be assumed, without loss of generality, that $v(z, \tau)$ has the following form

$$v(z, \tau) = V(z)e^{\lambda\tau} + \text{c.c.} \tag{23}$$

where λ is a complex constant, $V(z)$ is a complex-valued function, and c.c. denotes

the complex conjugate [28]. After substituting Eq. (23) into Eq. (22) we find

$$\mathcal{L}V = \lambda V.$$

This is now a differential eigenvalue problem with eigenvalue λ and eigenfunction V [6]. Floquet's theorem states that all bounded solutions to this equation have the form

$$V(z) = e^{i\mu z} \sum_{k=-\infty}^{\infty} \hat{v}(k) e^{\frac{ikz2\pi}{L}} = \sum_{k=-\infty}^{\infty} \hat{v}(k) e^{iz\left(\mu + \frac{2\pi k}{L}\right)}, \tag{24}$$

where $\hat{v}(k)$ are complex numbers and $\mu \in (-\frac{\pi}{L}, \frac{\pi}{L}]$ is a real constant called the Floquet parameter [6][10].

Substituting (24) into the dynamical system, and truncating, gives

$$\hat{\mathcal{L}}\hat{V} = \lambda \hat{V},$$

where $\hat{V} = (\hat{v}(-N), \hat{v}(-N+1), ..., \hat{v}(N-1), \hat{v}(N))^T$ is the vector of the coefficients $\hat{v}(k)$ from $k = -N$ to $k = N$. In order to determine the stability of the equilibrium solution we compute the eigenvalues λ of this truncated, formerly bi-infinite, square matrix for a range of values of μ. If the eigenvalues λ have zero real part, then the solution is said to be spectrally stable. If the eigenvalues do have a non-zero real part, this means that the perturbation grows exponentially, and the solution is spectrally unstable [6].

3.2 Cubic-Vortical Whitham equation

We now apply this theory to the specific example of the CV-Whitham equation. This was outlined by Carter et al. in [6] and more details were kindly provided to me in a personal communication from Carter. First apply the change of variables

$z = x - ct$ and $\tau = t$. This transforms the CV-Whitham equation from

$$\eta_t + \mathcal{K} * \eta_x + \alpha\eta\eta_x + \beta\eta^2\eta_x = 0 \tag{25}$$

to

$$\eta_\tau - c\eta_z + \mathcal{K} * \eta_z + \alpha\eta\eta_z + \beta\eta^2\eta_z = 0, \tag{26}$$

and transforms travelling wave solutions of the former (25) into stationary solutions of the latter (26).

To assess the stability of the stationary solutions (also known as equilibrium solutions), consider a stationary solution with an added perturbation, i.e.:

$$\eta_{pert}(z,\tau) = \eta(z) + \epsilon v(z,\tau) + O(\epsilon^2), \tag{27}$$

where η is the stationary solutions, v is the perturbation, and ϵ is a small positive constant. The ϵv term makes up the leading-order part of the perturbation.

The perturbed solution (27) is substituted into (26), linearised, and simplified to give

$$v_\tau - cv_z + \mathcal{K} * v_z + \alpha\eta v_z + \alpha\eta_z v + 2\beta\eta\eta_z v + \beta\eta^2 v_z = 0.$$

Applying the product rule in reverse, this equation simplifies the last four terms to

$$\begin{aligned} v_\tau - cv_z + \mathcal{K} * v_z + (\alpha\eta v)_z + (\beta\eta^2 v)_z &= 0 \\ v_\tau - cv_z + \mathcal{K} * v_z + [(\alpha\eta + \beta\eta^2)v]_z &= 0. \end{aligned} \tag{28}$$

This is an autonomous, in τ, nonlocal partial differential equation, and thus it can be assumed without loss of generality that

$$v(z,\tau) = V(z)e^{\lambda\tau} + \text{c.c.} \tag{29}$$

where V is a complex-valued function, λ is a complex constant, and c.c. denotes the

complex conjugate. Substituting (29) into (28) gives

$$cV' - \mathcal{K} * V' - \left[(\alpha\eta + \beta\eta^2)V\right]' = \lambda V \tag{30}$$

where prime denotes differentiation with respect to z. Using Floquet's Theorem we now assume that all bounded solutions to this equation have the form

$$V(z) = e^{i\mu z} \sum_{k=-\infty}^{\infty} \hat{v}(k) e^{\frac{ikz2\pi}{L}} = \sum_{k=-\infty}^{\infty} \hat{v}(k) e^{iz(\mu + \frac{2\pi k}{L})}. \tag{31}$$

Substituting (31) into (30) gives

$$c \sum_{k=-\infty}^{\infty} \hat{v}(k) i \left(\mu + \frac{2\pi k}{L}\right) e^{iz(\mu+\frac{2\pi k}{L})} - \mathcal{K} * \sum_{k=-\infty}^{\infty} \hat{v}(k) i \left(\mu + \frac{2\pi k}{L}\right) e^{iz(\mu+\frac{2\pi k}{L})} - \left[(\alpha\eta + \beta\eta^2)V\right]' = \lambda \left[\sum_{k=-\infty}^{\infty} \hat{v}(k) e^{iz(\mu+\frac{2\pi k}{L})}\right],$$

which simplifies to

$$\sum_{k=-\infty}^{\infty} \left[i \left(\mu + \frac{2\pi k}{L}\right) e^{iz\left(\mu+\frac{2\pi k}{L}\right)} \left(c - \mathcal{K}\left(\mu + \frac{2\pi k}{L}\right)\right) \hat{v}(k) \right] - \left[\left(\alpha\eta + \beta\eta^2\right) V\right]' = \lambda \left[\sum_{k=-\infty}^{\infty} \hat{v}(k) e^{iz\left(\mu+\frac{2\pi k}{L}\right)}\right].$$

For ease of notation, define $h(z)$

$$h(z) = \alpha\eta(z) + \beta\eta^2(z) \tag{32}$$

giving

$$\underbrace{\sum_{k=-\infty}^{\infty}\left[i\left(\mu+\frac{2\pi k}{L}\right)e^{iz\left(\mu+\frac{2\pi k}{L}\right)}\left(c-\mathcal{K}\left(\mu+\frac{2\pi k}{L}\right)\right)\hat{v}(k)\right]}_{1}-\underbrace{[h(z)V]'}_{2}$$

$$=\underbrace{\lambda\left[\sum_{k=-\infty}^{\infty}\hat{v}(k)e^{iz\left(\mu+\frac{2\pi k}{L}\right)}\right]}_{3} \tag{33}$$

with three separate terms labelled 1, 2 and 3. It is clear that Terms 1 and 3 include a multiplication by $e^{iz\left(\mu+\frac{2\pi k}{L}\right)}$. To see that the same is true for Term 2, recall the convolution that

$$f(x)\cdot g(x)=\sum_{k}\left(\hat{f}*\hat{g}\right)_k e^{ikt}$$

where

$$\left(\hat{f}*\hat{g}\right)_k=\sum_{n}\hat{f}(n)\hat{g}(k-n)=\sum_{n}\hat{f}(k-n)\hat{g}(n). \tag{34}$$

Term 2 is $[h(z)V]'$; using the assumption previously made from Floquet's theorem (31) and the Fourier expansion of $h(z)=\sum_{j=\infty}^{\infty}\hat{h}(j)e^{\frac{2\pi ijz}{L}}$, this term becomes

$$[h(z)V]'=\left[\left(\sum_{j=-\infty}^{\infty}\hat{h}(j)e^{\frac{2\pi ijz}{L}}\right)\left(\sum_{k=-\infty}^{\infty}\hat{v}(k)e^{iz\left(\mu+\frac{2\pi k}{L}\right)}\right)\right]'.$$

Using the convolution (34) we find

$$[h(z)V]'=\left[\sum_{k=-\infty}^{\infty}\left(\sum_{n=-\infty}^{\infty}\hat{h}(k-n)\hat{v}(n)\right)e^{iz\left(\mu+\frac{2\pi k}{L}\right)}\right]'.$$

Now take the derivative with respect to z to get:

$$\begin{aligned}[h(z)V]'&=\left[\sum_{k=-\infty}^{\infty}\left(\sum_{n=-\infty}^{\infty}\hat{h}(k-n)\hat{v}(n)\right)e^{iz\left(\mu+\frac{2\pi k}{L}\right)}i\left(\mu+\frac{2\pi k}{L}\right)\right]\\&=\left[\sum_{k=-\infty}^{\infty}i\left(\mu+\frac{2\pi k}{L}\right)\left(\sum_{n=-\infty}^{\infty}\hat{h}(k-n)\hat{v}(n)\right)e^{iz\left(\mu+\frac{2\pi k}{L}\right)}\right].\end{aligned}$$

Inserting this expression into Eq. (33), the result is

$$\sum_{k=-\infty}^{\infty}\left[i\left(\mu+\frac{2\pi k}{L}\right)e^{iz\left(\mu+\frac{2\pi k}{L}\right)}\left(c-\mathcal{K}\left(\mu+\frac{2\pi k}{L}\right)\right)\hat{v}(k)\right] - \left[\sum_{k=-\infty}^{\infty} i\left(\mu+\frac{2\pi k}{L}\right)\left(\sum_{n=-\infty}^{\infty}\hat{h}(k-n)\hat{v}(n)\right)e^{iz\left(\mu+\frac{2\pi k}{L}\right)}\right] = \lambda\left[\sum_{k=-\infty}^{\infty}\hat{v}(k)e^{iz\left(\mu+\frac{2\pi k}{L}\right)}\right].$$

The exponential term cancels out to get

$$\sum_{k=-\infty}^{\infty}\left[i\left(\mu+\frac{2\pi k}{L}\right)\left(c-\mathcal{K}\left(\mu+\frac{2\pi k}{L}\right)\right)\hat{v}(k)\right] - \sum_{k=-\infty}^{\infty} i\left(\mu+\frac{2\pi k}{L}\right)\left(\sum_{n=-\infty}^{\infty}\hat{h}(k-n)\hat{v}(n)\right) = \lambda\sum_{k=-\infty}^{\infty}\hat{v(k)}.$$

Therefore, for each $k\in\mathbb{Z}$ we have that

$$i\left(\mu+\frac{2\pi k}{L}\right)\left(c-\mathcal{K}\left(\mu+\frac{2\pi k}{L}\right)\right)\hat{v}(k) - i\left(\mu+\frac{2\pi k}{L}\right)\sum_{n=-\infty}^{\infty}\hat{h}(k-n)\hat{v}(n) = \lambda\hat{v}(k),$$

after reverting to the full expression for h (see Eq. (32)), we find

$$i\left(\mu+\frac{2\pi k}{L}\right)\left(c-\mathcal{K}\left(\mu+\frac{2\pi k}{L}\right)\right)\hat{v}(k) - i\left(\mu+\frac{2\pi k}{L}\right)\sum_{n=-\infty}^{\infty}\left(\alpha\hat{\eta}(k-n)+\beta\hat{\eta^2}(k-n)\right)\hat{v}(n) = \lambda\hat{v}(k).$$

The Fourier coefficients of η^2, denoted above by $\hat{\eta^2}$, are let equal $\hat{\zeta}$ for legibility, so

finally

$$i\left(\mu+\frac{2\pi k}{L}\right)\left(c-\mathcal{K}\left(\mu+\frac{2\pi k}{L}\right)\right)\hat{v}(k) - i\left(\mu+\frac{2\pi k}{L}\right)\sum_{n=-\infty}^{\infty}\left(\alpha\hat{\eta}(k-n)+\beta\hat{\zeta}(k-n)\right)\hat{v}(n) = \lambda\hat{v}(k). \tag{35}$$

Truncating this and putting it in matrix form, it can now be written as

$$\hat{\mathscr{L}}\hat{V}=\lambda\hat{V}$$

where $\hat{V}$ is the vector $\hat{V}=\left(\hat{V}(-N),\hat{V}(-N+1),...,\hat{V}(N)\right)^T$ and $\hat{\mathscr{L}}$ is the square matrix

$$\hat{\mathscr{L}}=\begin{cases} i\left(\mu+\frac{2\pi k}{L}\right)\left(c-\mathcal{K}\left(\mu+\frac{2\pi k}{L}\right)\right), \text{ for } k=n \\ i\left(\mu+\frac{2\pi k}{L}\right)\left(-\alpha\hat{\eta}(k-n)-\beta\hat{\zeta}(k-n)\right), \text{ for } k\neq n. \end{cases} \tag{36}$$

To visualise this transition from standard equation form (35) to matrix form (36), consider (35) for the case $k=3$

$$\underbrace{i\left(\mu+\frac{6\pi}{L}\right)\left(c-\mathcal{K}\left(\mu+\frac{6\pi}{L}\right)\right)\hat{v}(3)}_{\text{A}} \underbrace{- i\left(\mu+\frac{6\pi}{L}\right)\sum_{n=-\infty}^{\infty}\left(\alpha\hat{\eta}(3-n)+\beta\hat{\zeta}(3-n)\right)\hat{v}(n)}_{\text{B}} = \lambda\hat{v}(3).$$

The term A only appears on the diagonal of the matrix $\hat{\mathscr{L}}$, i.e. when $k=n$, because this term is only multiplied by $\hat{v}(3)$. If it occurred elsewhere, in addition to the diagonal, this term would be multiplied by the entire vector $\hat{v}(n)$, rather than just the single element $\hat{v}(3)$ of the vector.

The term B is multiplied by $\hat{v}(n)$, so it arises in every element of the matrix $\hat{\mathscr{L}}$.

However, in the $\beta = 0$ case, on the diagonal where $n = k$, $\hat{\eta}(n-k) = \hat{\eta}(0)$; because we only consider solutions with zero mean $\hat{\eta}(0) = 0$, and the B term falls away here on the diagonal. In the $\beta \neq 0$ case, i.e. where $\hat{\zeta}$ is included, $\hat{\zeta} = \hat{\eta^2}$ and if η has zero mean then η^2 is positive and $\hat{\eta^2}(0) = \hat{\zeta}(0) \neq 0$, and we must include the B term in the matrix. In this case, use (35) over (36).

Note on the Whitham equation: The same derivation can be repeated for the standard Whitham equation, rather than the CV-Whitham equation. The classical Whitham equation is the same as the CV-Whitham equation with $\beta = 0$ (to remove the cubic term) and $\Omega = 0$ (which will give $\alpha = \frac{3}{2}$ and ensure the kernel term $\mathcal{K}$ from the CV-Whitham equation becomes equal to the kernel term K from the classical Whitham equation). Letting the coefficient of the nonlinear term be α, the derivation follows the above discussion closely, starting with

$$\eta_t + K * \eta_x + \alpha\eta\eta_x = 0.$$

This gives the same $\hat{\mathscr{L}}$ for the classical Whitham equation as one would determine from setting $\beta = 0$ in the result from the CV-Whitham equation. The only difference in the derivation is that $h(z)$ will be defined as $h(z) = \alpha\eta(z)$ rather than $h(z) = \alpha\eta(z) + \beta\eta(z)$, i.e. the $\beta = 0$ case.

Note on the computation: Mathematically, $\hat{\eta}$ and $\hat{\zeta}$ are bi-infinite vectors and $\hat{\mathscr{L}}$ is a bi-infinite matrix. This cannot be dealt with numerically and the expressions are truncated at a suitable size. After this truncation, the vectors, as well as rows and columns of the matrix, are indexed from $-N$ to N. The central element has index zero, which is normal for bi-infinite vectors. Although vectors and matrices are no longer infinite, this indexing system is grandfathered in and remains after truncation. Illustrated below is an example where $N = 2$, producing the 5×5 matrix

with rows n and columns k, and elements a indexed by their rows and columns.

$$\begin{array}{c} \begin{array}{ccccc} \text{-2} & \text{-1} & 0 & 1 & 2 \end{array} \\ \begin{pmatrix} a_{-2,-2} & a_{-2,-1} & a_{-2,0} & a_{-2,1} & a_{-2,2} \\ a_{-1,-2} & a_{-1,-1} & a_{-1,0} & a_{-1,1} & a_{-1,2} \\ a_{0,-2} & a_{-0,-1} & a_{0,0} & a_{0,1} & a_{0,2} \\ a_{1,-2} & a_{1,-1} & a_{1,0} & a_{1,1} & a_{1,2} \\ a_{2,-2} & a_{2,-1} & a_{2,0} & a_{2,1} & a_{2,2} \end{pmatrix} \end{array} \begin{array}{c} \text{-2} \\ \text{-1} \\ 0 \\ 1 \\ 2 \end{array}$$

After truncating, $\hat{\eta}$ and $\hat{\zeta}$ are vectors of size $2N+1$, and $\hat{\mathscr{L}}$ is an $(2N+1)\times(2N+1)$ matrix. Note that in the code, the indexing runs from 1 to $2N+1$, because one cannot have negative indices in most programming languages.

In (36) the $k \neq n$ case requires evaluation of $\hat{\eta}(k-n)$ and $\hat{\zeta}(k-n)$. However, due to the truncation, some of the highest and lowest possible indices of these vectors do not exist, i.e. they lie outside the bounds of the vectors. Taking the example above, the element $a_{2,-2}$ of the matrix would require the element $\hat{\eta}(2-(-2)) = \hat{\eta}(4)$ of the vector, however, the indexing of $\hat{\eta}$ only extends as high as 2. In the example above, the same is also true for $a_{1,-2}$, $a_{2,-1}$, $a_{-2,1}$, $a_{-2,2}$, and $a_{-1,2}$. Therefore, where these "corner" values of the matrix require vector elements outside the valid range, the truncation sets them to zero.

4 CV-Whitham equation computational results

The method for determining the solutions of the CV-Whitham equation was given in Section 2.6.4, and the method for determining those solutions' stability was given in Section 3.2. This section compiles and discusses computational results using these methods.

The solutions to the CV-Whitham equations were found for $\Omega = 0$ with the period $L = 2\pi$, and for several different values of the wave speed c. The initial value used for c was $\mathcal{K}(\frac{2\pi}{L}) = \mathcal{K}(1) = 0.872694$ [6]. The initial guess given to the root finder was that $\hat{f}(1) = 0.1$ and $\hat{f}(k) = 0$ for $k = 2, ..., N$. After the first iteration, the solution found was used as the next initial guess, and the value of c was incremented, and later also decremented, slowly.

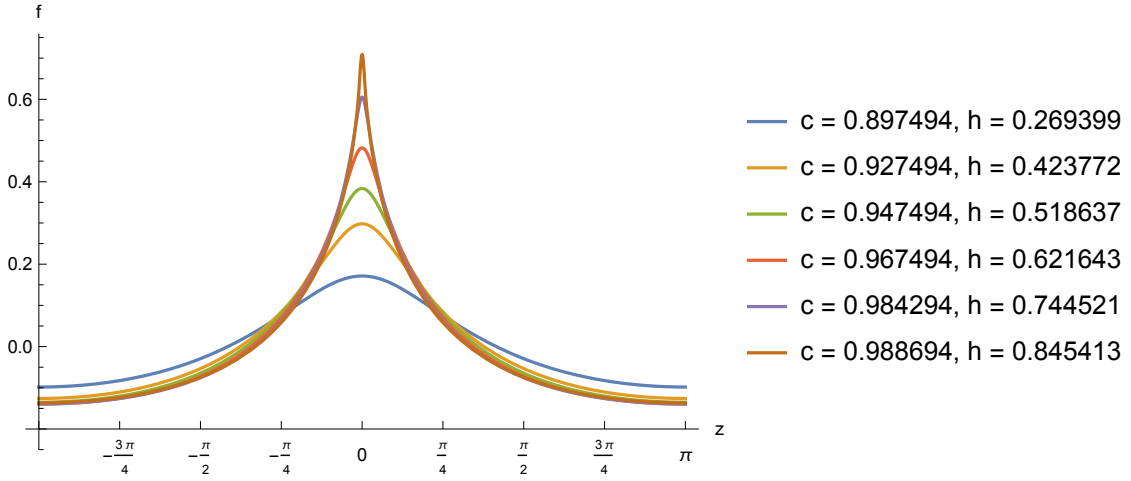


Figure 6: Solutions to the CV-Whitham equation with $L = 2\pi$, $\Omega = 0$, and various values of wave speed c. The calculated wave height of the solution is also given.

Figure 6 depicts some of the solutions found, including the wave speed and wave height of that solution. The wave height H is calculated as the difference between the maximum and minimum values of the solution. From this figure, it can be seen that the wave height increases as the wave speed increases. The solutions with smaller wave speeds, and therefore wave heights, are smooth and sinusoidal in nature; whilst

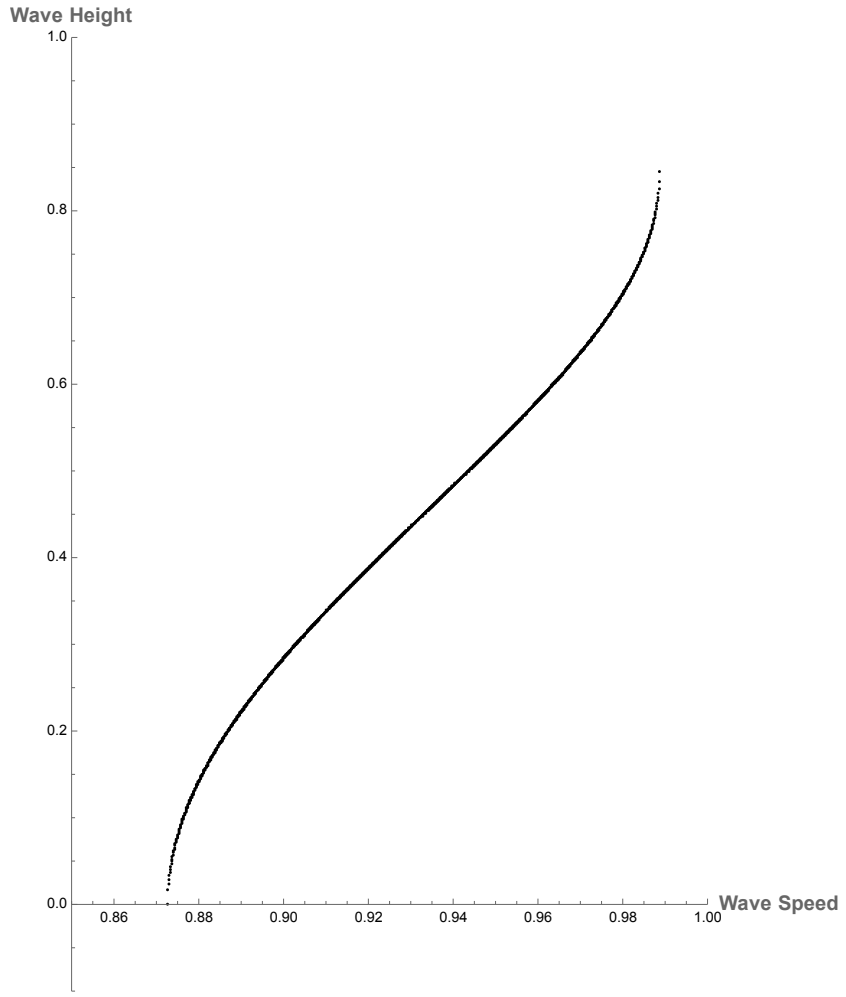
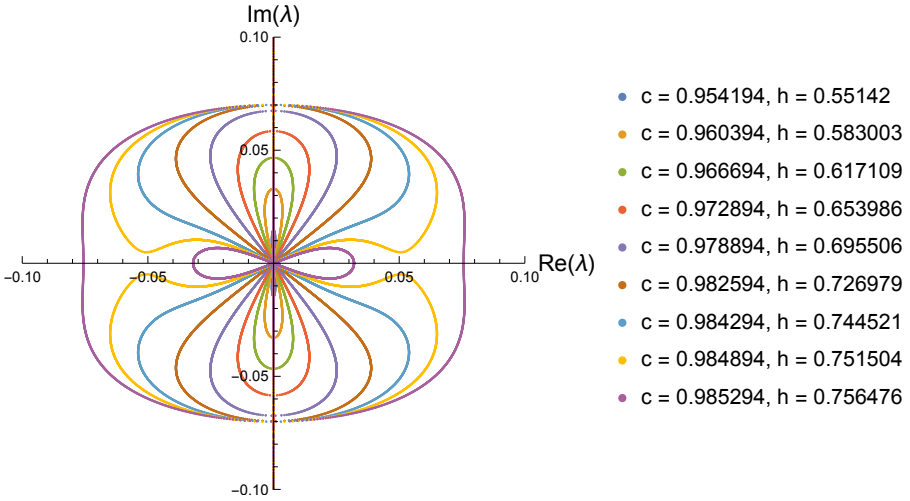


Figure 7: Plot of wave speed c versus wave height H for solutions of the CV-Whitham equation with $L = 2\pi$ and $\Omega = 0$.

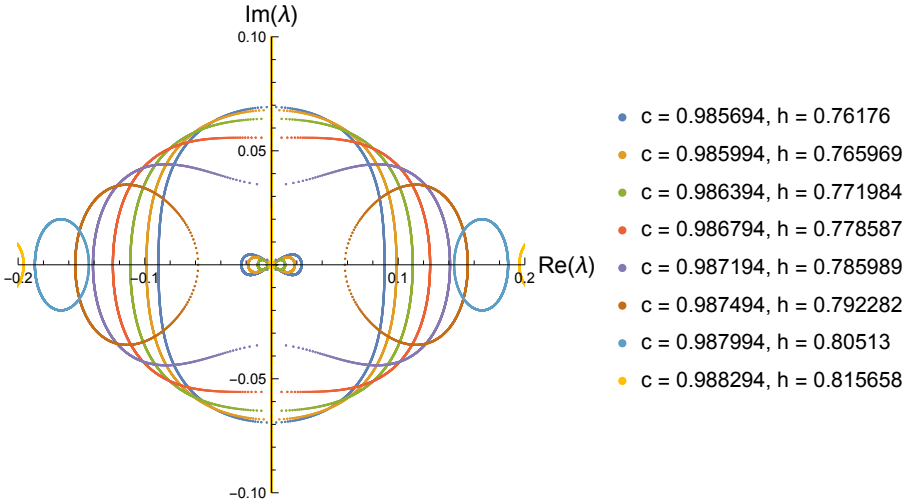
solutions at higher wave speeds and wave heights tend to become more peaked with increasingly steep sides. This is consistent with Carter et al.'s results in [6]. It is better visualised in Figure 7, where the wave speed c is plotted against the wave height H for a large number of solutions. The solutions range from wave speeds of $0.872694 \leq c \leq 0.988694$, with values of c below this range yielding no solution, and values of c above this range yielding double-peaked solutions with decreasing eigenvalues that are thought to be untrue. The solutions used to make this figure were found with 128 Fourier modes.

Additionally, for both $L = \pi$ and $L = 2\pi$, Carter et al. [6] gave representative

solutions with $\Omega = 0, \pm 0.2, \pm 0.4, \pm 0.6, \pm 0.8, \pm 1.0$, where, for each Ω, the solutions for multiple values of the wave speed c are given. For each set of solutions for a given Ω, they found the same pattern: increasing wave speed gave solutions of increased wave height and steeper slopes surrounding the peak. They state that, for each L and Ω, there appeared to be a solution of maximal wave height. They include bifurcation curves for multiple values of Ω for a larger range of c, finding that the maximal wave height increases as Ω decreases.



(a)



(b)

Figure 8: Stability spectra for some solutions of the CV-Whitham equation with $L = 2\pi$ and $\Omega = 0$, where it is not enforced that the mean is zero, with their respective wave speeds c and wave heights h given.

Figure 8 shows the stability spectra of solutions for a variety of wave speeds. All solutions have a line of purely imaginary eigenvalues forming a vertical line along the y-axis. Unstable solutions also have positive real parts, whereas stable solutions are exclusively restricted to the imaginary axis. A positive real part indicates that the corresponding perturbation grows exponentially, hence giving rise to the instability. All solutions found for values of c less than 0.952494 were shown to be stable, with no non-zero real parts of the eigenvalues, which is consistent with existing research by Carter et al. [6]. Figure 8 shows the spectra of some of the unstable solutions to the CV-Whitham equation, with Figure 8a demonstrating the "figure eight" shape characteristic of modulational instability, while for solutions with larger wave heights the spectra forms a "figure infinity" surrounded by an oval. In Figure 8b, which shows stability spectra for solutions with further increasing values of c, the "figure infinity" is seen to decrease in size, while the surrounding oval slowly splits into two ovals on the x-axis. These results are also in keeping with the results of Carter et al. [6]. Using a finer incrementation of the Floquet parameter μ will give a denser plot, however is a huge increase in the amount of computation required. These plots were made by incrementing μ from -0.5 to 0.5 in steps of 0.001.

Figure 9 shows the maximum real part of the eigenvalues λ for the solutions found. The solution is stable where the maximum real part of the eigenvalue is zero, i.e. the curve lies on the x-axis. In Figure 9, the curve lies on the x-axis, i.e. where the eigenvalues λ have no non-zero real part, indicating their stability. At $c = 0.952494$ the maximum of the real parts of the eigenvalues becomes non-zero, and steadily increases as wave speed increases, indicating stronger instability. For this calculation, an eigenvalue greater than 10^{-10} is considered to be non-zero.

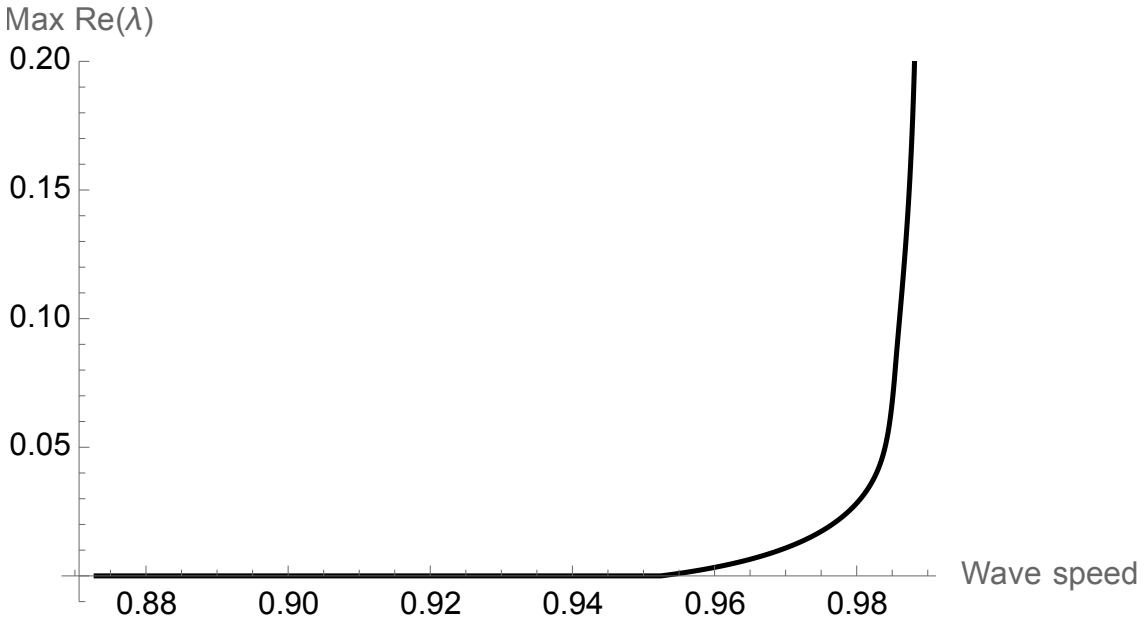


Figure 9: Wave speed c versus the maximum real eigenvalue of the stability spectra, for solutions to the CV-Whitham equation with $L = 2\pi$ and $\Omega = 0$.

5 Modified Dispersion Whitham equation

Wave breaking refers to a solution in which the slope becomes vertical (attempting to overturn as seen in nature). The solution ceases to exist because it becomes multi-valued. In his book [31], Whitham notes that the KdV equation will never give solutions that break, due to the dispersive effect of the third derivative term. On the other hand, nonlinear shallow water equations without dispersive effects are dominated by the nonlinear term, and therefore result in breaking solutions. Whitham posed the question: is there a simple model that yields both continuous and breaking solutions? In response, Whitham suggested what is now known as the Whitham equation. In this equation the dispersive third derivative term of the KdV equation is replaced with a kernel,

$$\eta_t + \frac{3}{2}\eta\eta_x + K * \eta_x = 0.$$

The kernel we have considered thus far is that originally proposed by Whitham, namely

$$\hat{K}(k) = \sqrt{\frac{\tanh(k)}{k}}.$$

To model both breaking and continuous waves, Mortell and Mulchrone [25] proposed a nonlocal kernel, which will be explored in more detail in the next section.

5.1 Derivation

In [25], Mortell and Mulchrone seek a kernel giving both continuous and breaking solutions and begin with the observation that

$$\eta_{xxx} \equiv \int_{-\infty}^{\infty} \delta''(x)\eta_\xi d\xi, \tag{37}$$

which, if considered in the context of the KdV equation, means that when searching for a replacement for the third derivative term one might be well served by finding a function that approximates the delta function δ, taking its second derivative, and substituting that in (37) in place of $\delta''(x)$. They use a Gaussian function $f(x) = ae^{-bx^2}$ with $b = \pi a^2$ as such an approximation of δ. This choice of b ensures that $\int_{-\infty}^{\infty} f(x)dx \equiv 1$, which is a crucial property of the delta function. Letting $a = \frac{\nu^2}{\sqrt{\pi}}$ gives that

$$f(x) = \frac{\nu^2}{\sqrt{\pi}} e^{-\nu^4 x^2}, -\infty < x < \infty. \tag{38}$$

Lighthill [22] makes the following two definitions, firstly (p.15, Defn. 1) that

Definition 5.1 *A **good function** is one which is everywhere differentiable any number of times and such that it and all its derivatives are $\mathcal{O}(|x|^{-N})$ as $|x| \mapsto \infty$ for all N.*

Secondly, he states (p.17, Defn. 5) that

Definition 5.2 *A **generalised function** $f(x)$ is defined as a regular sequence $f_n(x)$ of good functions, but two generalised functions are said to be equal if the corresponding regular sequences are equivalent. Thus, each generalised function is really the class of all regular sequences equivalent to a given regular sequence. [...]*

In [25], it is noted that $f(x) = \frac{\nu^2}{\sqrt{\pi}} e^{-\nu^4 x^2}$ is a good function. Additionally, $f(x)$ has the following properties:

- Firstly, it was chosen such that it has zero mean, i.e. $\int_{-\infty}^{\infty} f(x)dx = 1$,
- Secondly, is has a maximum at $x = 0$, with $f(0) = \frac{\nu^2}{\sqrt{\pi}}$, where the limit of $f(0)$ as ν goes to infinity is infinity, i.e. $\lim_{\nu \to \infty} f(0) = \infty$, and
- Thirdly, it is equal to the Gaussian $\mathcal{N}(0, \frac{1}{\sqrt{2}\nu^2})$, the variance of which goes to zero as ν goes to infinity, i.e. $\lim_{\nu \to \infty} \frac{1}{\sqrt{2}\nu^2} = 0$.

Therefore, the sequence $g_n(x) = \frac{n^2}{\sqrt{\pi}} e^{-n^4 x^2}$ with $\int_{-\infty}^{\infty} g_n(x)dx = 1$ is a regular se-

quence, and $\lim_{n\to\infty} g_n(x)F(x)dx$ exists for any good function $F(x)$.

With a proof that follows Lighthill's work, Mortell and Mulchrone (Thm. 2.1 [25]) give that

Theorem 5.1 [25] The sequence $\frac{n^2}{\sqrt{\pi}}e^{-n^4x^2}$ defines a generalised function $\delta(x)$ such that $\int_{-\infty}^{\infty}\delta(x)F(x)dx = F(0)$, where $F(x)$ is a good function. [...]

Proof: See Lighthill [22].

Wherefrom, using that $\frac{\nu^2}{\sqrt{\pi}}e^{-\nu^4x^2}$ is by Lighthill's definition equivalent to $\frac{n^2}{\sqrt{\pi}}e^{-n^4x^2}$, we have that

$$\lim_{\nu\to\infty}\frac{\nu^2}{\sqrt{\pi}}e^{-\nu^4x^2} = \delta(x).$$

In other words, for high values of ν, (38) is a good approximation of the delta function. Taking the second derivative of (38) defines our kernel in the spatial domain:

$$\frac{d^2}{dx^2}\left(\frac{\nu^2}{\sqrt{\pi}}e^{-\nu^4x^2}\right) = \frac{2\nu^6}{\sqrt{\pi}}\left(2\nu^4x^2-1\right)e^{-\nu^4x^2} = K(x).$$

To find the Fourier transform $\hat{K}(k)$ of $K(x)$ take

$$\begin{aligned}\hat{K}(k) &= \int_{-\infty}^{\infty}K(x)e^{-ikx}dx\\ &= \int_{-\infty}^{\infty}\frac{2\nu^6}{\sqrt{\pi}}\left(2\nu^4x^2-1\right)e^{-\nu^4x^2}e^{-ikx}dx\\ &= \frac{4\nu^{10}}{\sqrt{\pi}}\underbrace{\int_{-\infty}^{\infty}x^2e^{-\nu^4x^2}e^{-ikx}dx}_{\text{A}} - \frac{2\nu^6}{\sqrt{\pi}}\underbrace{\int_{-\infty}^{\infty}e^{-\nu^4x^2}e^{-ikx}dx}_{\text{B}}.\end{aligned}$$

The integral B is the Fourier transform of a Gaussian function, which is known to be

$$\mathcal{F}\{e^{-ax^2}\} = \sqrt{\frac{\pi}{a}}e^{-\frac{k^2}{4a}},$$

while the integral A is the Fourier transform of the product of a polynomial and a

Gaussian function, which is known to be

$$\mathcal{F}\{x^n e^{-ax^2}\} = (-i)^n \sqrt{\frac{\pi}{a}} \left(\frac{d^n}{dk^n} e^{-\frac{k^2}{4a}} \right).$$

Hence, using these substitutions and having calculated the necessary second derivative,

$$\hat{K}(k) = \frac{4\nu^{10}}{\sqrt{\pi}} \left(\left(-\frac{\sqrt{\pi}k^2}{4\nu^{10}} + \frac{\sqrt{\pi}}{2\nu^6} \right) e^{-\frac{k^2}{4\nu^4}} \right) - \frac{2\nu^6}{\sqrt{\pi}} \left(\frac{\sqrt{\pi}}{\nu^2} e^{-\frac{k^2}{4\nu^4}} \right)$$

which simplifies quickly to

$$\hat{K}_\nu(k) = -k^2 e^{-\frac{k^2}{4\nu^4}}. \tag{39}$$

The subscript ν is included to distinguish this kernel from those discussed earlier and indicates that this kernel includes the tuneable parameter ν. For higher values of ν, such as 2π, the function $f(x)$, defined in (38), is a very close approximation of the delta function, and therefore $K_\nu * \eta_x$ is close to the dispersion term of the KdV equation. For lower values of ν, the function $f(x)$, given in (38), is a poorer representation of the delta function and has less of an effect, as it grows increasingly nonlocal with a smoother peak. In summary, for high values of ν this model is close to the KdV equation, and for lower values of ν the model is close to shallow water theory. This model is referred to as the Modified Dispersion Whitham (or MD-Whitham) equation, as it allows for change in the strength of the dispersion term to yield different solutions.

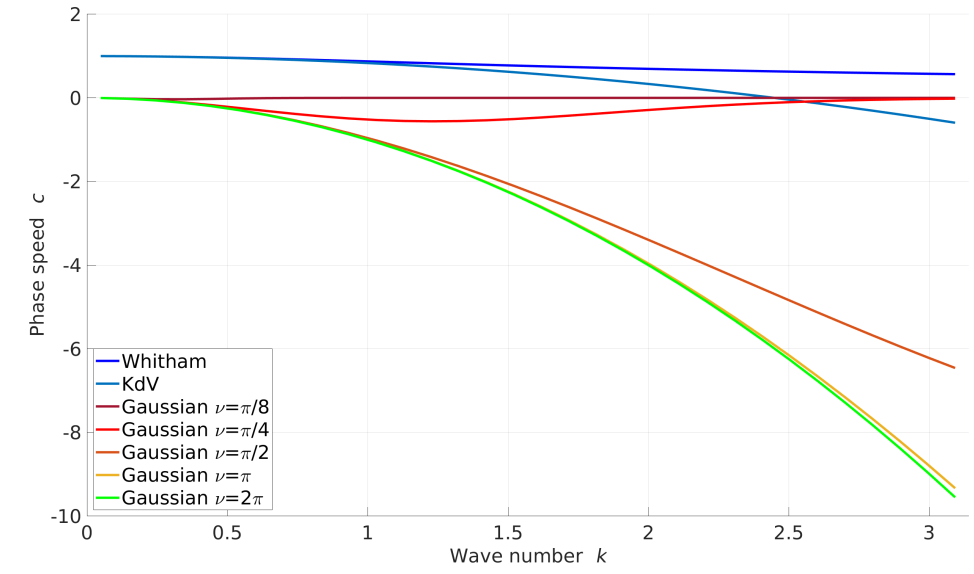
5.2 Comparison between linear phase speed of kernels

The dispersive terms used so far are

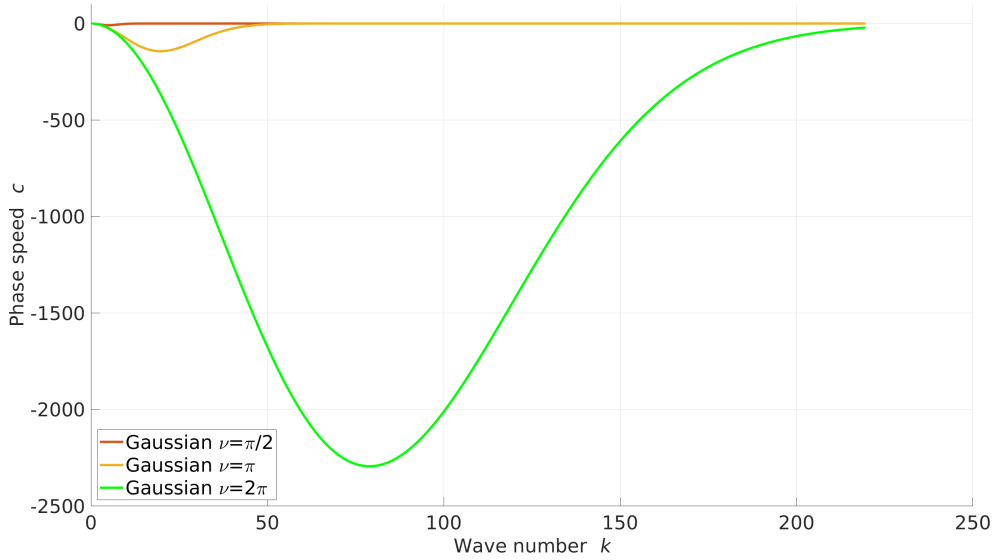
- the third derivative term of the KdV equation,
- the kernel $\hat{K}(k)$ from the Whitham equation, defined in (14),
- the CV-Whitham kernel $\hat{\mathcal{K}}(k)$ defined in (17), which when $\Omega = 0$ is equivalent

to $\hat{K}(k)$ of the Whitham equation above (the only case considered here), and

- the nonlocal kernel $\hat{K}_\nu(k)$ defined in (39).



(a)



(b)

Figure 10: Plot of the linear phase speed $\tilde{c}$ against the wave number k for the Whitham, KdV, and MD-Whitham models, the latter done for values of $\nu = 2\pi, \pi, \frac{\pi}{2}, \frac{\pi}{4}, \frac{\pi}{8}$.

According to Sanford et al., the dispersive term dictates the linear phase speed $\tilde{c}$ of the model [28]. In the case of the KdV equation, this is $\tilde{c} = 1 - \frac{1}{6}k^2$, which is found by taking the first two terms in the Taylor expansion of $\sqrt{\frac{\tanh(k)}{k}}$ around $k = 0$ [28]. The linear phase speed of the Whitham equation is $\tilde{c} = \sqrt{\frac{\tanh(k)}{k}}$, and for the MD-Whitham model is $\tilde{c} = -k^2 e^{-\frac{k^2}{4\nu^4}}$. Figure 10 compares these visually, for several different values of ν in the MD-Whitham case. In Figure 10a it can be seen that the Whitham phase speed is the most flat, while the phase speed for the KdV equation falls lower. For all values of ν the MD-Whitham model's phase speed starts at zero, experiences a dip, and then returns to zero. For $\nu = \frac{\pi}{8}$, the dip is imperceptibly small using this scaling. For $\nu = \frac{\pi}{2}$, π, 2π, though they are included in Figure 10a, it takes the scaling on Figure 10b to see that they too eventually return to zero.

5.3 Solution results

We seek solutions to the following Whitham-type equation,

$$\eta_t + \frac{3}{2}\eta\eta_x + K_\nu * \eta_x = 0$$

with the nonlocal kernel,

$$\hat{K}_\nu(k) = -k^2 e^{-\frac{k^2}{4\nu^4}}.$$

This is the MD-Whitham equation. This equation is equivalent to the CV-Whitham equation with some minor changes:

- Firstly, the kernel $\mathcal{K}$ defined by (17) must be replaced by K_ν defined in (39),
- Secondly, if $\Omega = 0$ then $\alpha = \frac{3}{2}$ and $\beta = -\frac{3}{8}$; for the MD-Whitham equation, $\Omega = 0$ and $\alpha = \frac{3}{2}$, however, we take $\beta = 0$ to remove the cubic vortical term.

The same solution method used for the CV-Whitham equation is applied to the MD-Whitham equation and the details are not repeated.

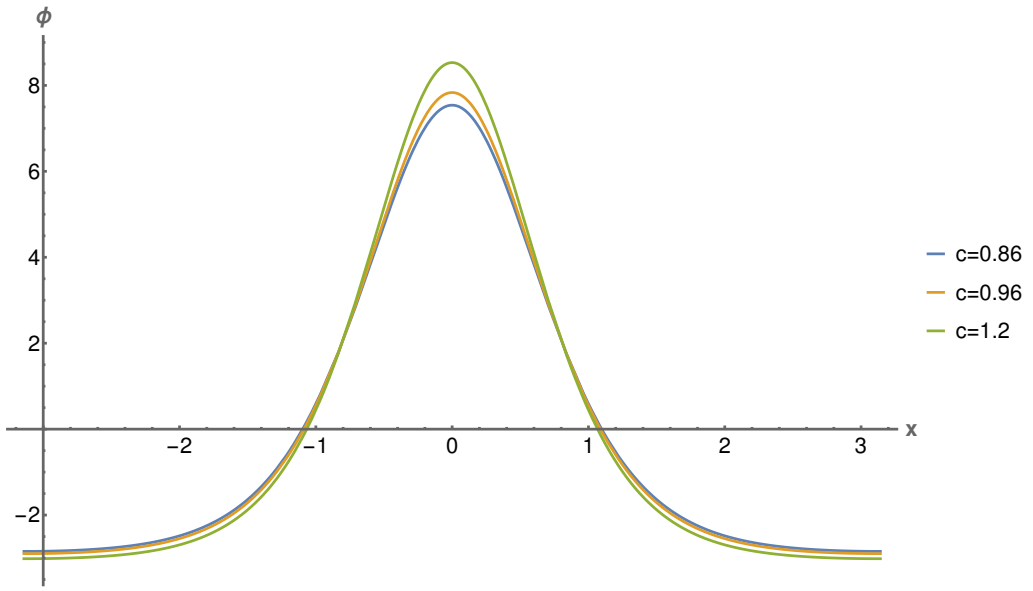


Figure 11: Solutions to the Whitham equation with a nonlocal kernel for $\nu = 2\pi$

To begin with we took $\nu = 2\pi$ because at this value the Dirac delta function is approximated reasonably well (see Section 5.1). Consequently, we expect the MD-Whitham equation to be similar to the KdV equation at this value. A solution with wave speed $c = 1.2$ was sought first. Our initial guess for the solution (for use with Newton's method), was a solution to the KdV equation found earlier, i.e. similar to that given in Figure 2a. Solutions for other wave speeds were found by incrementing or decrementing c by a small amount. The initial guess for the new value of c was taken to be the solution for the previous value of c. Having established solutions for $\nu = 2\pi$ we then sought solutions for different values of ν. A similar approach was taken, that is, as the value of ν was decremented by a small amount the initial guess was the solution found previously for the same value of c and the old value of ν.

Figures 11, 12, and 13 show solutions to the Whitham equation with this nonlocal kernel for $\nu = 2\pi$, $\frac{3\pi}{2}$, and π respectively, for three representative values of c.

While the change in c lead to differences in the wave height of the solution, changing ν seems to have relatively little visible effect. However, the results are only given in the figures until $\nu = \pi$. Even though the initial guesses ought to have been

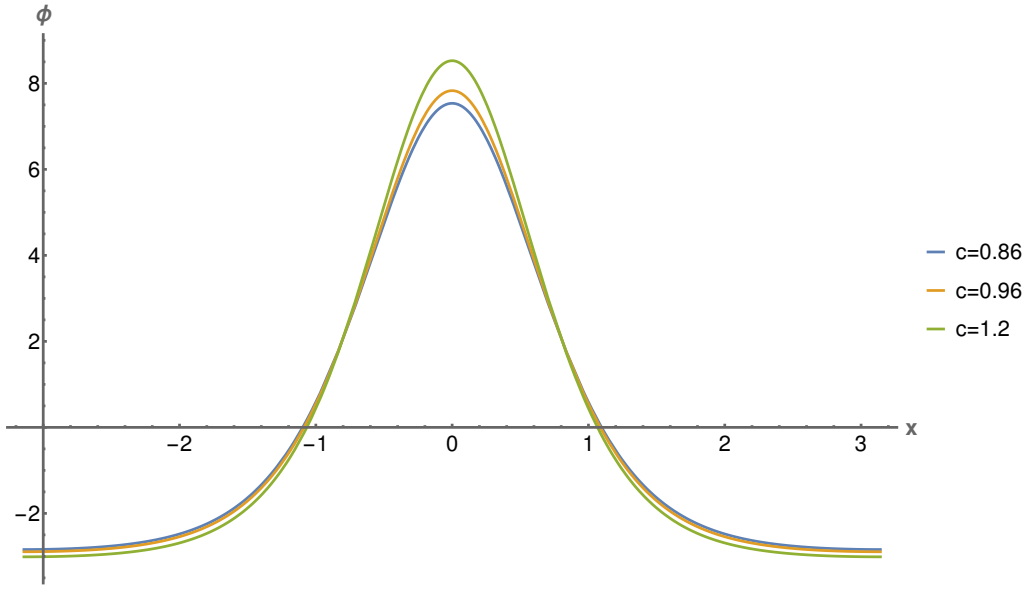


Figure 12: Solutions to the Whitham equation with a nonlocal kernel for $\nu = \frac{3\pi}{2}$

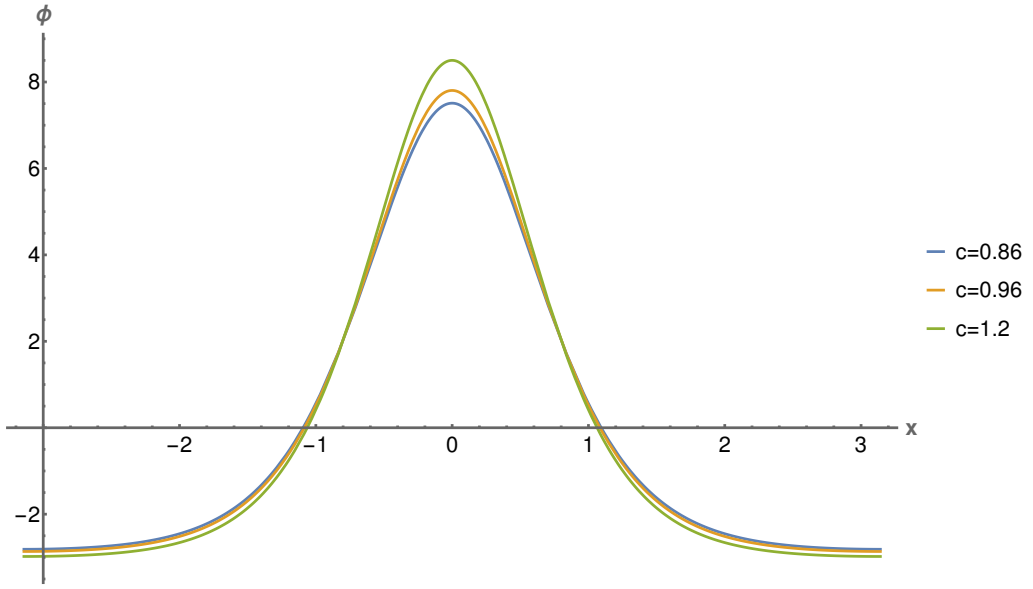


Figure 13: Solutions to the Whitham equation with a nonlocal kernel for $\nu = \pi$

close, the root finder converged to zero solutions at approximately $\nu = \frac{7\pi}{8}$. When $c = 1.2$ and $\nu \geq \frac{29\pi}{32}$ it still converged to nontrivial solutions, and then failed to do so when $\nu \leq \frac{57\pi}{64}$. This cut-off value has some dependency on c though, because when $c = 0.85$, it still converged to nontrivial solutions when $\nu = \frac{57\pi}{64}$, and only failed to do so when $\nu = \frac{7\pi}{8}$. For these experiments, ν was decremented in steps of size $\frac{\pi}{64}$. Further reduction of the stepsizes of c and ν did not prevent it from converging to the zero solution, but would increase the precision of the cut-off point.

This convergence to a zero solution is not entirely surprising when comparing the solution method with the anticipated numerical results. With a model that mimics the KdV equation for high values of ν, symmetrical results like those shown in Figures 11, 12, and 13 are anticipated and obtained. For lower values of ν, the reduction of the dispersive effect allows the nonlinear term to dominate and create an asymmetrical solution. Naturally, a Fourier method based on the assumption of an even solution falls short here. Therefore it is unsurprising that for values of ν where breaking and asymmetrical solutions are expected, the numerical method fails to converge to a nontrivial solution.

5.4 Spectral stability results

The stability analysis that was carried out for the CV-Whitham equation was also carried out for the non-zero solutions of the MD-Whitham equation.

The eigenvalue equations equivalent to (35) and (36) for the CV-Whitham equation are found by noting that the only differences are that $\alpha = \frac{3}{2}$, $\beta = 0$, and the nonlocal kernel K_ν is now used in place of $\mathcal{K}$. Therefore, the full eigenvalue equation

is

$$i\left(\mu+\frac{2\pi k}{L}\right)\left(c-K_\nu\left(\mu+\frac{2\pi k}{L}\right)\right)\hat{v}(k) - i\left(\mu+\frac{2\pi k}{L}\right)\sum_{n=-\infty}^{\infty}\left(\frac{3}{2}\hat{\eta}\left(k-n\right)\right)\hat{v}(n) = \lambda\hat{v}(k),$$

which, truncated and with the same stipulations as before, is written in matrix form as

$$\hat{\mathscr{L}}\hat{V}=\lambda\hat{V},$$

where $\hat{V}$ is the vector $\hat{V}=\left(\hat{V}(-N),\hat{V}(-N+1),...,\hat{V}(N)\right)^T$ and $\hat{\mathscr{L}}$ is the square matrix

$$\hat{\mathscr{L}}=\begin{cases} i\left(\mu+\frac{2\pi k}{L}\right)\left(c-K_\nu\left(\mu+\frac{2\pi k}{L}\right)\right), & \text{for } k=n \\ i\left(\mu+\frac{2\pi k}{L}\right)\left(-\frac{3}{2}\hat{\eta}(k-n)\right), & \text{for } k\neq n. \end{cases}$$

The eigenvalues of $\hat{\mathcal{L}}$ were determined for a number of solutions, and all the solutions were found to be stable. The stability spectra had no real part and consisted exclusively of imaginary terms. This can be seen for the $\nu=2\pi$, $c=1.2$ solution in Figure 14. The stability spectra of all other solutions were identical, and for brevity are omitted.

It is important to make the distinction that while all the solutions found seem to be stable, that does not mean that all the solutions to the MD-Whitham kernel are stable. Due to the assumption of even-ness inherent in the solution method, only symmetrical solutions were found.

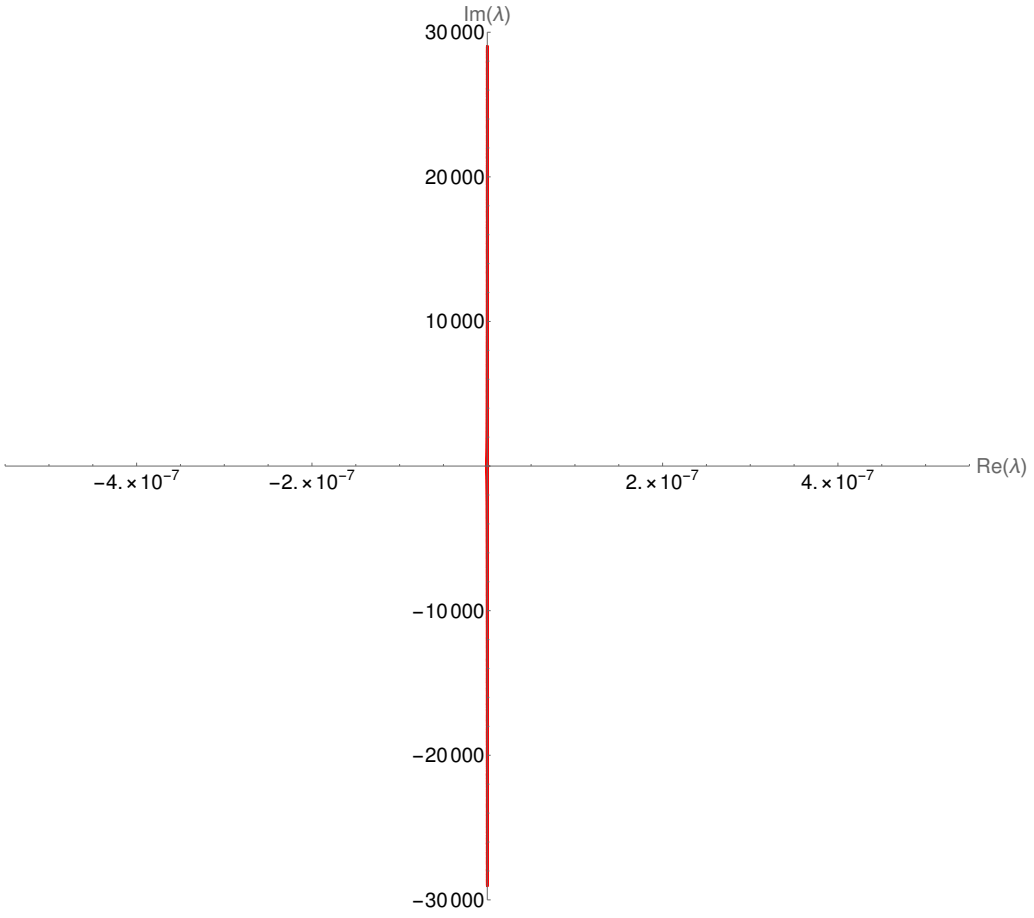


Figure 14: Stability spectra of the representative solution to the MD-Whitham term for $\nu = 2\pi$ and $c = 1.2$.

6 Discussion and Conclusion

6.1 Discussion

In Brunton and Kutz' book (Ch. 2.3, [5]), the Burgers equation is solved to give asymmetrical solutions by using a Fast Fourier Transform (FFT) to transform into the Fourier domain where the first and second derivatives are computed, and then transforming back into the spatial domain to compute the nonlinear product. This gives a system of ODEs which can be solved using any suitable ODE solver. Trying this method may allow asymmetrical, i.e. not even, solutions to the MD-Whitham equation, which the current solution method prohibits.

To demonstrate this method first consider an easier, linear example such as the heat equation

$$u_t = \alpha^2 u_{xx}$$

where $u(x,t)$ is the temperature at the point x and time t. When transformed into the Fourier domain, i.e. $\mathcal{F}(u(x,t)) = \hat{u}(\kappa,t)$, the wavelengths or spatial frequencies κ are a vector. The derivative with respect to time is transformed from u_t to $\hat{u}_t$, but the important advantage of the transformation is that the derivative with respect to x in Fourier space is given by

$$u_x \Rightarrow i\kappa\hat{u}$$
$$u_{xx} \Rightarrow (i\kappa)^2\hat{u} = -\kappa^2\hat{u}.$$

Therefore, rather than considering a PDE in the spatial domain, the problem has been transformed into a system of ODEs in the Fourier domain:

$$\hat{u}_t = -\alpha^2\kappa^2\hat{u},$$

which can be solved using an ODE solver, and the solution then transformed back

into the spatial domain. The solution to the Heat equation, using a square hat function as the initial condition, can be seen progressing over time in Figure 15.

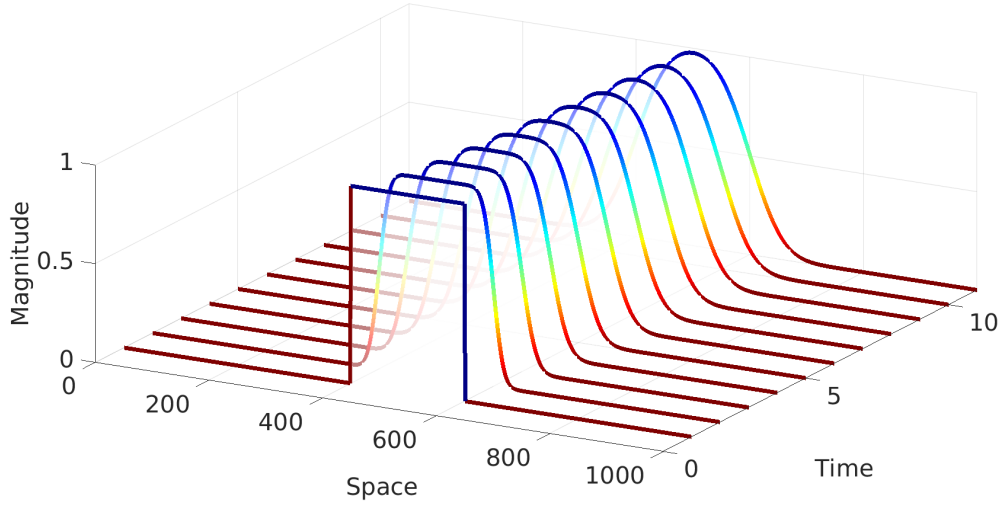


Figure 15: Solution to the Heat equation progressing over time, found in the method described by Kutz and Brunton [5].

A nonlinear, and therefore slightly more convoluted, example is that of the Burgers equation, which, as before, is given by

$$\eta_t + \eta\eta_x = \epsilon\eta_{xx}.$$

This can be rewritten as

$$\eta_t = \epsilon\eta_{xx} - \eta\eta_x,$$

which, using the FFT, transforms into the system of ODEs

$$\hat{\eta}_t = \epsilon(-\kappa^2\hat{\eta}) - \hat{\eta}(i\kappa\hat{\eta}).$$

This simplifies to

$$\hat{\eta}_t = -\epsilon\kappa^2\hat{\eta} - i\kappa\hat{\eta}^2.$$

While the transformation to Fourier space has again greatly simplified the calculation of the derivatives, in the earlier example the heat equation could, at this point,

be solved in the Fourier domain and the solution transformed back to the spatial domain. In this example, this system of ODEs cannot be easily solved in the Fourier domain, due to the presence of the nonlinear term. Therefore, the system of ODEs must now be transformed back into the spatial domain, where it can be solved. To be clear, the difference between the two examples is in whether the system is solved in the Fourier domain and the solution then transformed into the spatial domain, or whether the entire system of ODEs is transformed back into the spatial domain, where its solution can then be found. The latter method is obviously less computationally efficient, but it remains sufficiently efficient, and is necessary in cases where a nonlinear term is present.

The solutions found for the Burger's example are plotted over time in Figure 16, where they can be seen to be asymmetrical solutions.

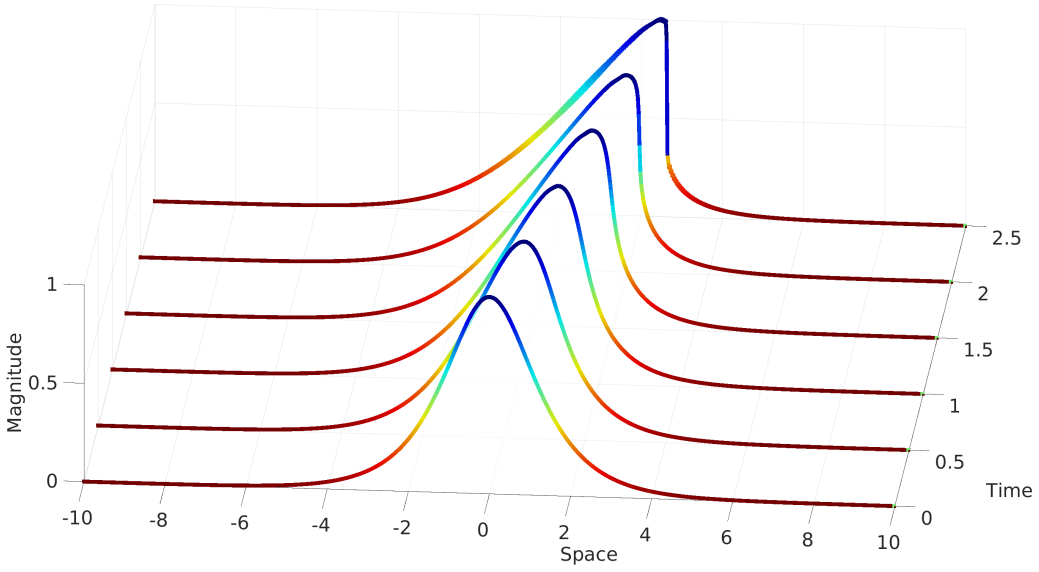


Figure 16: Solution to the Burgers equation progressing over time, found in the method described by Brunton and Kutz [5].

Using this same method, Figure 17 shows time iterated solutions to the MD-Whitham equation for $\nu = \frac{\pi}{16}$. This shows that steepness does increase and the system approaches breaking solutions for low values of ν.

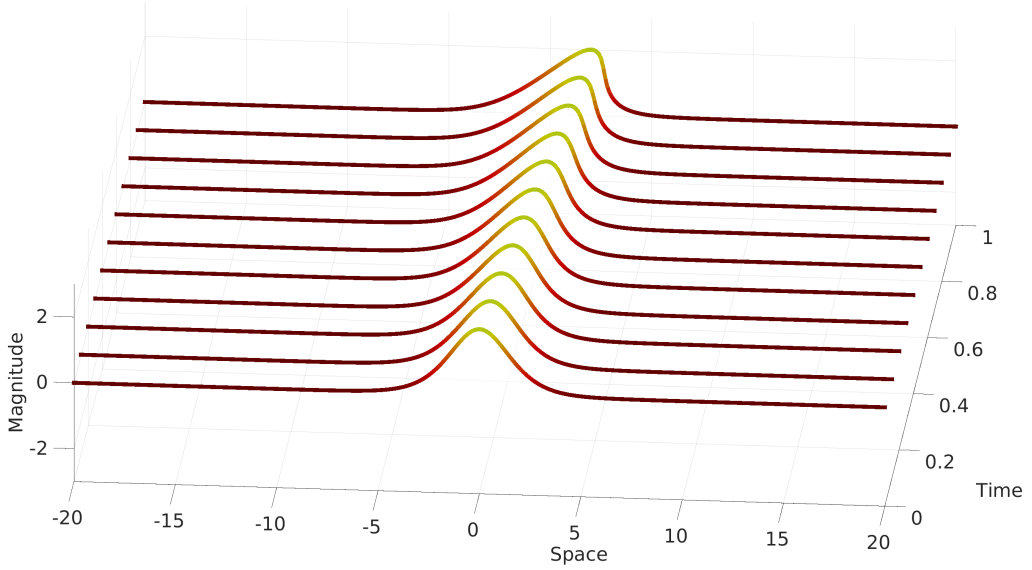


Figure 17: Solutions to the MD-Whitham equation for $\nu = \frac{\pi}{16}$ progressing over time, found in the method described by Brunton and Kutz [5]

For such nonlinear models with reduced or zero diffusion the wave speed at a point on the solution becomes proportional to the amplitude at that point. Where the solution is higher in amplitude it moves forwards faster, causing increasing steepness until a shock front forms. Regardless of the numerical technique used to solve this, at the shock front, where the solution ceases to be a function as it attempts to become multi-valued, the computation will fail. However, one can come close to seeing the breaking solutions when the right side has become very steep, but not yet infinitely steep. Further work is required to carry out the stability analysis of these solutions and determine if they are spectrally stable or unstable.

In particular this work involves

- Adding a Burgers term to the Modified Dispersion Whitham equation i.e.

$$\eta_t + \frac{3}{2}\eta\eta_x + K_\nu * \eta_x = \epsilon\eta_{xx}.$$

The Burgers term softens the shock solution such that even though the wave

becomes asymmetrical the steepness reaches a finite value. Hence we may expect stable asymmetric solutions.

- Modifying the solution method by removing the *a priori* assumption of an even solution. For this purpose we suggest that the solution method described in Section 2.7 is best suited, whereby the assumption that $\hat{f}(-k) = \hat{f}(k)$ is removed.

- Finding solutions and running the spectral stability analysis.

6.2 Conclusion

In summary, in this thesis we have studied a process of finding solutions to certain PDEs and then determining the stability of those solutions. We began by introducing spectral methods, and the differences between spectral methods, finite element methods, and finite difference methods, before introducing the spectral cosine collocation method that can be used to solve the equations of interest. For this, the discrete cosine transform and its inverse were derived, as well as differentiation matrices. The Korteweg-deVries-Burgers equation, and its dichotomised subparts the Korteweg-deVries equation and the Burgers equation, as well as the Whitham, Whitham-Burgers, and cubic vortical Whitham equation were introduced, with their relevant histories, uses, and limitations. These were then solved using the method outlined above, and the cubic vortical Whitham equation was solved again using an alternative method detailed by Carter et al. [6]. These solutions were all consistent with prior work by Nevland [26], and Sanford et al. [28].

Thereafter, with solutions found and the intent to determine their stability, the Fourier-Floquet-Hill method was introduced. A description of the method and its history was given, before its application to the CV-Whitham equation was detailed, with a few notes on the computations thereof and the equivalence of the method on the Whitham equation. The solutions of the CV-Whitham equation and their

stability analysis was included, and was consistent with prior work done by Carter et al. It was found that increased wave speed led to increased wave height, and that for lower wave speeds solutions were found to be stable, while for higher wave speeds, the solutions were unstable.

Finally, we introduced a nonlocal kernel as an alternative dispersion term, the MD-Whitham equation. The purpose of this was to provide a model that yields both breaking and continuous solutions. The continuous solutions were found, and the solution method was determined inadequate to find the breaking solutions, due to the inherent assumption in the method that the solution be even. A more suitable method might be a time-evolution method used by Brunton and Kutz [5] to show asymmetrical solutions to the Burgers equation, and this would be a good starting point for future work. The stability analysis of the continuous solutions gave that they were stable for approximately $\nu > \frac{7\pi}{8}$. We only found zero or trivial solutions for values of ν less than this. The expectation is that continuous solutions would be found to be stable, while breaking solutions would be found to be unstable. The former has been found to be true, and the latter part requires a modified method for finding solutions before their stability can be assessed. For future work, it would be also be fascinating to see what precisely happens to the stability in the transition from continuous to breaking solutions; it is possible that some solutions which have only mildly increasing steepness remain stable, and there is a threshold level of nonlinearity that causes the solution to become unstable.

References

[1] Bona, J., & Schonbek, M. (1985). Travelling-wave solutions to the Korteweg-deVries-Burgers equation. *Proceedings of the Royal Society of Edinburgh Section A: Mathematics*, *101*(3-4), 207–226.

[2] Boussinesq, J. (1877). *Essai sur la théorie des eaux courantes*. Impr. nationale. https://gallica.bnf.fr/ark:/12148/bpt6k56673076.texteImage

[3] Bradie, B. (2006). *A friendly introduction to numerical analysis*. Pearson Education India.

[4] Brillouin, L. (1946). Wave propagation in periodic structures. *McGraw-Hill Book Company*, *2*, 2022–2025.

[5] Brunton, S. L., & Kutz, J. N. (2022). *Data-driven science and engineering: Machine learning, dynamical systems, and control*. Cambridge University Press.

[6] Carter, J. D., Kalisch, H., Kharif, C., & Abid, M. (2022). The cubic vortical Whitham equation. *Wave Motion*, *110*, 102883.

[7] Casperson, L. W. (1984). Solvable Hill equation. *Phys. Rev. A*, *30*, 2749–2751. https://doi.org/10.1103/PhysRevA.30.2749

[8] Costa, B. (2004). Spectral methods for partial differential equations. *CUBO, A Mathematical Journal*, *6*(4), 1–32. http://revistas.ufro.cl/ojs/index.php/cubo/article/view/1552

[9] Darrigol, O. (2017). Joseph Boussinesq's legacy in fluid mechanics [A century of fluid mechanics: 1870–1970]. *Comptes Rendus Mécanique*, *345*(7), 427–445. https://doi.org/10.1016/j.crme.2017.05.008

[10] Deconinck, B., & Kutz, J. N. (2006). Computing spectra of linear operators using the Floquet–Fourier–Hill method. *Journal of Computational Physics*, *219*(1), 296–321.

[11] Ehrnström, M., & Kalisch, H. (2009). Traveling waves for the Whitham equation. *Differ. Int. Equations*, *22*, 1193–1210. https://doi.org/10.57262/die/1356019412

[12] Folland, G. (2009). *Fourier analysis and its applications*. American Mathematical Society. https://books.google.ie/books?id=ix2iCQ-o9x4C

[13] Gerry, C., & Knight, P. (2004). *Introductory quantum optics*. Cambridge University Press.

[14] Hill, G. W. (1886). On the part of the motion of the lunar perigee which is a function of the mean motions of the sun and moon.

[15] Hur, V. M. (2017). Wave breaking in the whitham equation. *Advances in Mathematics*, *317*, 410–437.

[16] Hur, V. M., & Johnson, M. A. (2015). Modulational instability in the Whitham equation for water waves. *Studies in Applied Mathematics*, *134*(1), 120–143.

[17] Hur, V. M., & Tao, L. (2018). Wave breaking in a shallow water model. *SIAM Journal on Mathematical Analysis*, *50*(1), 354–380. https://doi.org/10.1137/15M1053281

[18] Kharif, C., & Abid, M. (2018). Nonlinear water waves in shallow water in the presence of constant vorticity: A Whitham approach. *European Journal of Mechanics-B/Fluids*, *72*, 12–22.

[19] Kharif, C., Abid, M., & Touboul, J. (2017). Rogue waves in shallow water in the presence of a vertically sheared current. *Journal of Ocean Engineering and Marine Energy*, *3*, 301–308.

[20] Korteweg, D. J., & de Vries, G. (1895). XLI. On the change of form of long waves advancing in a rectangular canal, and on a new type of long stationary waves. *The London, Edinburgh, and Dublin Philosophical Magazine and Journal of Science*, *39*(240), 422–443. https://doi.org/10.1080/14786449508620739

[21] Koutserimpas, T. T., & Fleury, R. (2018). Electromagnetic waves in a time periodic medium with step-varying refractive index. *IEEE Transactions on Antennas and Propagation*, *66*(10), 5300–5307. https://doi.org/10.1109/TAP.2018.2858200

[22] Lighthill, M. J. (1958). *An introduction to Fourier analysis and generalised functions*. Cambridge University Press.

[23] Martini, M. (1996). *An introduction to transverse beam dynamics in accelerators* (tech. rep.).

[24] Moldabayev, D., Kalisch, H., & Dutykh, D. (2015). The Whitham equation as a model for surface water waves. *Physica D: Nonlinear Phenomena*, *309*, 99–107.

[25] Mortell, M. P., & Mulchrone, K. F. (2021). Numerical study of a Whitham equation exhibiting both breaking waves and continuous solutions. *AIP Advances*, *11*(4).

[26] Nevland, M. (2022). *Nonlocal models for undular bores* [Master's thesis, The University of Bergen].

[27] Russell, J. S. (1845). *Report on waves: Made to the meetings of the british association in 1842-43*.

[28] Sanford, N., Kodama, K., Carter, J. D., & Kalisch, H. (2014). Stability of traveling wave solutions to the Whitham equation. *Physics Letters A*, *378*(30-31), 2100–2107.

[29] Sheretov, E. P. (2000). Opportunities for optimization of the RF signal applied to electrodes of quadrupole mass spectrometers.: Part I. General theory. *International Journal of Mass Spectrometry*, *198*(1), 83–96. https://doi.org/https://doi.org/10.1016/S1387-3806(00)00165-2

[30] Stacey, A. (2011, November). The Azimuth project: Spectral methods for PDEs. https://web.archive.org/web/20180206085851/azimuthproject.org/azimuth/show/Spectral+methods+for+PDEs

[31] Whitham. (1974). *Linear and nonlinear waves*. John Wiley & Sons.

[32] Zabusky, N. J., & Kruskal, M. D. (1965). Interaction of "solitons" in a collisionless plasma and the recurrence of initial states. *Phys. Rev. Lett.*, *15*, 240–243. https://doi.org/10.1103/PhysRevLett.15.240

7 Appendices

7.1 Mathematica code to solve the CV-Whitham equation and determine the stability of those solutions

```
SolveEquation[L_, Omega_, c_, Num_, init_] := Module[{alpha, beta, i,
   eqs, ics, res},
  alpha = Omega^2 + 3/Sqrt[Omega^2 + 4];
  beta = -(6 + Omega^2)/(2 (Sqrt[4 + Omega^2]^3));
  eqs = Table[MakeEquation[i, c, Omega, alpha, beta, L, Num], {i, 1,
    Num}];
  ics = Table[{f1, init[[i]]}, {i, 1, Num}];
  res = FindRoot[eqs, ics];
  {Table[If[i != 0, res[Abs[i], 2], 0], {i, -Num, Num}], Table[res[i,
    2], {i, 1, Num}]}
]
```

```
Kern[x_, Omega_] := Module[{res},
  If[x == 0,
   res = 1/2 (-Omega + Sqrt[4 + Omega^2]);,
   res = -(Omega Tanh[x])/(2 x) + Sqrt[Tanh[x]/x + (Omega^2 Tanh[x]^2)
   /(4 x^2)
       ];
   ];
  res
  ]
```

```
MakeEquation[k_, c_, Omega_, alpha_, beta_,
  L_, Num_] := Module[{eq, l, j, rules},
  eq = -c  Subscript[f, k] + Kern[2 Pi k/L, Omega] Subscript[f,k] +
   alpha/2 Sum[Subscript[f, k - l] Subscript[f, l], {l, Max[-Num, -Num
    + k], Min[Num, Num + k]}] + beta/3 Sum[Sum[Subscript[f, k - j]
   Subscript[f, j - l] Subscript[f, l], {l, Max[-Num, -Num + j], Min[
   Num, Num + j]}], {j, Max[-2 Num, -Num + k], Min[2 Num, Num + k]}]
   == 0 // N;
```

```
  rules = Join[Table[Subscript[f, -i] -> Subscript[f, i], {i, 1, Num}],
    {Subscript[f, 0] -> 0}];
  eq /. rules
  ]
```

```
laurentCoefficientList[lpol_, x_] :=
 With[{min = Exponent[lpol, x, Min]}, CoefficientList[lpol/x^min, x]]
```

```
GetUSquared[fvals_] :=
 Module[{Num, i, ff, x, cl, f, Numd2, w, Numcl},
  Num = Length[fvals]; Numd2 = Quotient[Num, 2];
  f = Sum[fvals[[i + Numd2 + 1]] x^i, {i, -Numd2, Numd2}];
  ff = f f // Expand;
  cl = laurentCoefficientList[ff, x];
  Numcl = Length[cl];
  w = Table[cl[[i]], {i, 1 + Numd2, Numcl - Numd2}];
  w
  ]
```

```
ComputeMatrix[ifvals_, c_, Omega_, L_, mu_, wvals_] :=
 Module[{Num, fvals, i, k, rules, alpha, beta, Mat, Numd2, kvec,
    m, n, findex, kbar, nbar},
  alpha = Omega^2 + 3/Sqrt[ Omega^2 + 4];
  beta = -(6 + Omega^2)/(2 (Sqrt[4 + Omega^2]^3));
  Num = Length[ifvals]; Numd2 = Quotient[Num, 2];
  fvals = Table[ifvals[[i]], {i, 1, Num}];
  kvec = Table[i, {i, -Numd2, Numd2}];
  Mat = Table[0, {n, 1, Num}, {k, 1, Num}];
  For[k = -Numd2, k <= Numd2, k++,
   For[n = Max[-Numd2, -Numd2 + k], n <= Min[Numd2, Numd2 + k], n++,
     kbar = k + Numd2 + 1; nbar = n + Numd2 + 1;
     Mat[[nbar, kbar]] -=
        I (mu + 2 Pi k/L) (alpha fvals[[kbar - nbar + Numd2 + 1]]
        + beta wvals[[kbar - nbar + Numd2 + 1]]);
     If[nbar == kbar, Mat[[nbar, kbar]] += I (mu + 2 Pi k/L)
     (c - Kern[mu + 2 Pi k/L, Omega])];
     ];
```

```
   ];
  Mat
  ]
```

```
PlotEquation[fvals_, L_] :=
 Module[{eq, i, rules, Num, Numd2},
  Num = Length[fvals];
  Numd2 = Quotient[Num, 2];
  Sum[fvals[[i + Numd2 + 1]] Exp[2 Pi/L I i x], {i, -Numd2, Numd2}]
  ]
```

```
GoThroughSolutions[Num_, from_, to_] :=
 Module[{ic, i, j = 1, c, out, eq, hmax, output = {}, tot},
  (* size of arrays are 2 Num+1 *)
  tot = (to - from)/0.0001;
  ic = Table[0, {i, 1, Num}]; ic[[1]] = 0.1;
  Monitor[
   For[c = from, c < to, c += 0.0001,
     out = SolveEquation[2 Pi, 0, c, Num, ic];
     eq = PlotEquation[out[[1]], 2 Pi];
     hmax = ( Re[eq] /. x -> 0) - (Re[eq] /. x -> Pi);
     ic = out[[2]];
     AppendTo[output, {{c, hmax}, out[[1]]}];
     j++;
     ];,
   Row[{ProgressIndicator[j, {1, tot}], j}, " "]
   ];
  output
  ]
```

```
AppendUSquared[data_] := Module[{Num, w, i, tmp},
  Num = Length[data];
  tmp = data;
  For[i = 1, i <= Num, i++,
   w = GetUSquared[tmp[[i, 2]]];
   AppendTo[tmp[[i]], w];
   ];
```

```
  tmp
  ]
```

```
StoreEigenValues[data_, from_, to_] :=
 Module[{Num, c, h, maxreig, minreig, output = {}, j = 0, i, mu,
   eigs, tmp, sowdata},
  Num = Length[data];
  output = ParallelTable[
    c = data[[i, 1, 1]];
    h = data[[i, 1, 2]];
    eigs = Table[Eigenvalues[ComputeMatrix[data[[i, 2]], c, 0, 2 Pi,
        mu, data[[i, 3]]]], {mu, -.5, .5, .001}];
    tmp = Flatten[Join[eigs, Conjugate[eigs]]];
    maxreig = Max[Re[tmp]];
    minreig = Min[Re[tmp]];
    {{c, h, maxreig, minreig}, tmp}
    , {i, from, to}
    ];
  output
  ]

```

After all the functions have been defined, define the initial guess:

```
ic2 = Table[0, {i, 1, 32}];
ic2[[1]] = 0.1;
```

Defining the starting value of c, which is $\mathcal{K}(\frac{2\pi}{L}) = K(1)$:

```
konekern = Kern[1, 0] // N
```

Iterating through solutions, so the solution is found using the initial guess defined above, c is incremented, and then the solution is found for the new value of c using the previous solution as the new initial guess. This is slow to run, so it is only run once and the results exported:

```
res = GoThroughSolutions[32 , konekern + 0.005, konekern + 0.205]
```

```
Export["/home/katie/Documents/Uni/Masters/Assorted Mathematica code/
    Outputs/res2000.mx", res]
```

Computing, for each solution, the $\hat{\mathcal{L}}$ matrix and its eigenvalues, exporting all the eigenvalues for each solution, as well as exporting a matrix of wave speed, wave height, and the maximum real eigenvalue:

```
j = 1;
end = 2002;
graphdat = {};
Monitor[
  For[count = 1, count < end, count += 1,
    wvals = GetUSquared[res[[count, 2]]];
    eigs =
    Table[Eigenvalues[
      ComputeMatrix[res[[count, 2]], res[[count, 1, 1]], 0,
       2 Pi, mu, wvals]], {mu, -0.5, 0.5, 0.001}];
    alleigs = Flatten[Join[eigs, Conjugate[eigs]]];
    c = res[[count, 1, 1]];
    h = res[[count, 1, 2]];
    maxreig = Max[Re[alleigs]];
    relvals = {c, h, maxreig};
    AppendTo[graphdat, relvals];
    Export[
    StringJoin[
     "/home/katie/Documents/Uni/Masters/Assorted Mathematica code/
    Outputs/alleigs_results/alleigs", TextString[count], ".mx"],
    alleigs];
    Export[
    StringJoin[
     "/home/katie/Documents/Uni/Masters/Assorted Mathematica code/
    Outputs/relvals_results/relvals", TextString[count], ".mx"],
    relvals];
    Export[
    "/home/katie/Documents/Uni/Masters/Assorted Mathematica code/
    Outputs/graphingdata.mx", graphdat];
```

```
    j++;
    ];,
Row[{ProgressIndicator[j, {1, (end - 1)/1}], j}, ""]
]
```

7.2 Details on integration

Included here is some expounding information on the derivations performed in Section 2.6.1 and Section 2.6.2. In particular, this appendix aims to address why after integrating in both derivations a constant of integration was not included. This is closely related to the work done by Bona and Schonbek, and further details can be found in their paper [1].

In seeking a solution to the KdV-B equation, which Bona and Schonbek take as

$$u_t + uu_x + \delta u_{xxx} - \epsilon u_{xx} = 0,$$

they write the unique bounded solution as $\phi = \phi(\xi; \epsilon, \delta)$, where $\xi = x - ct$ (i.e. the travelling wave ansatz). Suppressing the dependence on the fixed values of ϵ and δ in the notation, this is often simply written as $\phi(\xi)$. The function ϕ, therefore, satisfies the equation

$$-c\phi' + \phi\phi' + \delta\phi''' - \epsilon\phi'' = 0, \tag{40}$$

where $'$ denotes differentiation with respect to ξ. Additionally, ϕ must also satisfy

$$\phi_L = \lim_{\xi \to -\infty} \phi(\xi), \text{ and}$$
$$\phi_R = \lim_{\xi \to +\infty} \phi(\xi),$$

as well as

$$\lim_{|\xi| \to +\infty} \phi^{(j)}(\xi) = 0, j = 1, 2, 3... \tag{41}$$

where $\phi^{(j)}$ denotes the j-th derivative with respect to $\xi = x - ct$ and the two asymptotic states ϕ_L and ϕ_R are restricted by the requirements that $c > \phi_R$ and $\phi_L + \phi_R = 2c$. Bona and Schonbek go into worthwhile detail on the geometry of the solutions in both the case where dispersion dominates, and where dissipation dominates, i.e. depending on the relative sizes of ϵ and δ, but it is not relevant to what we wish to clarify in this appendix. In seeking a solution ϕ that satisfies the conditions above, normalise ϕ by defining

$$\varphi(\xi) = \phi(\xi) - \phi_R.$$

Hence it follows that

$$-(c - \phi_R)\varphi' + \varphi\varphi' + \delta\varphi''' - \epsilon\varphi'' = 0,$$

which with the definition $\gamma = c - \phi_R$, gives an equation that has the same form as (40) with γ in place of c, namely

$$-\gamma\varphi' + \varphi\varphi' + \delta\varphi''' - \epsilon\varphi'' = 0. \tag{42}$$

The limiting conditions at infinity for φ are

$$\lim_{\xi\to-\infty} \varphi(\xi) = \varphi_0 = \phi_L - \phi_R, \quad \text{and} \quad \lim_{\xi\to+\infty} \varphi(\xi) = 0. \tag{43}$$

The conditions

$$\lim_{|\xi|\to+\infty} \varphi^{(j)}(\xi) = 0, j = 1, 2, 3...$$

correspond to (41), and also actually follow from (42) and (43), see Bona and Schonbek for further detail [1]. If φ, φ' and φ'' vanish at $+\infty$, then integrating (42) over $[y, \infty)$, gives that (42) is equivalent to

$$-\gamma\varphi(y) + \frac{1}{2}\varphi^2(y) + \delta\varphi''(y) - \epsilon\varphi'(y) = 0.$$